

# **Homogeneous antibody fragment conjugation by disulfide bridging introduces 'spinostics'**

Felix F Schumacher, Vishal A Sanchania, Berend Tolner, Zoë V F Wright, Chris P Ryan, Mark E B Smith, John M Ward, Stephen Caddick, Christopher W M Kay, Gabriel Aepli, Kerry A Chester & James R Baker

Correspondence should be addressed to J.R.B ([j.r.baker@ucl.ac.uk](mailto:j.r.baker@ucl.ac.uk)).

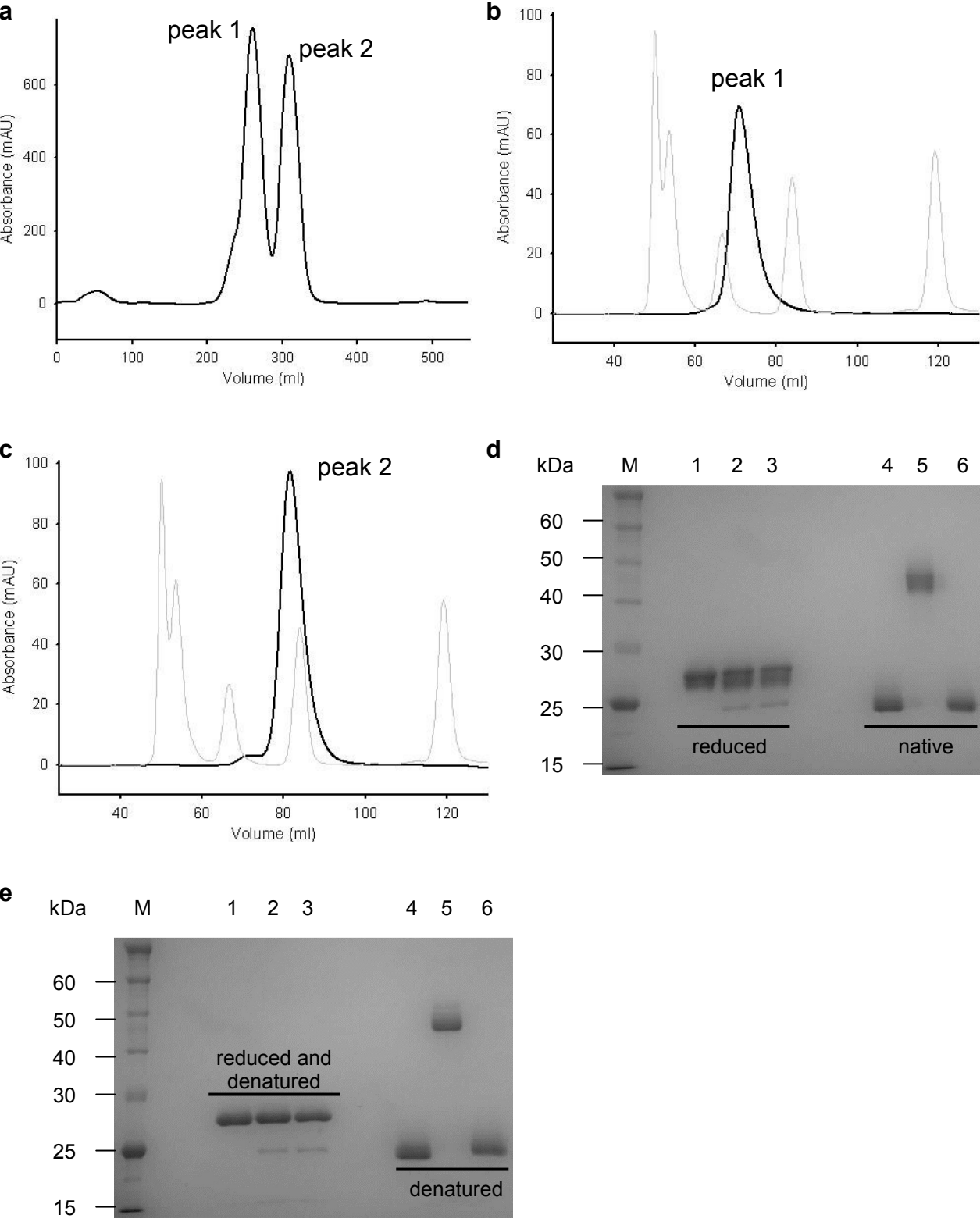
## Index

<b>Supplementary Figures</b> .....	<b>4</b>
Supplementary Figure S1: Purification of the sscFv .....	4
Supplementary Figure S2: FPLC analysis of variously bridged sscFv .....	6
Supplementary Figure S3: <i>In situ</i> bridging of the sscFv .....	7
Supplementary Figure S4: Optimization of the <i>in situ</i> protocol .....	8
Supplementary Figure S5: Mild chemical synthesis of N-functionalized maleimides .....	9
Supplementary Figure S6: Functionalisation of the sscFv.....	10
Supplementary Figure S7: Stability of sscFv analogues in human plasma .....	12
Supplementary Figure S8: Preparation and purification of HRP-sscFv conjugate .....	14
Supplementary Figure S9: Activity of the HRP-sscFv conjugate .....	15
Supplementary Figure S10: Specificity of the EPR-monitored binding event.....	16
Supplementary Figure S11: 10 $\mu$ M MP-sscFv and M <sub>C</sub> P-sscFv EPR spectra and simulated spectra	17
Supplementary Figure S12: MP- and M <sub>C</sub> P-sscFv EPR spectra in sucrose .....	24
Supplementary Figure S13: 250 nM MP-sscFv and M <sub>C</sub> P-sscFv EPR spectra and simulated spectra .....	25
Supplementary Figure S14: MP- and M <sub>C</sub> P-sscFv and MP- and M <sub>C</sub> P-sscFv-SM3E with and without NA1 thermal denaturation .....	30
Supplementary Figure S15: First derivative thermal denaturation fits .....	33
Supplementary Figure S16: Full-length gels .....	34
Supplementary Table S1: Rotational correlation times extracted by simulation and K <sub>d</sub> values extracted using least squares fitting .....	35
Supplementary Table S2: Thermal denaturation melting temperatures and enthalpies of unfolding	36
Supplementary Equation S1: Law of mass action fitting function .....	37
Supplementary Equation S2: Thermal denaturation fitting function.....	38
<b>Supplementary Methods</b> .....	<b>39</b>
General Methods.....	39
Reduction study of the sscFv .....	39
FPLC analysis of the sscFv.....	39
ELISA with the sscFv and its analogues .....	40
Biacore measurements .....	40
Synthesis of alkylated sscFv .....	40
Stability of bridged sscFv in human plasma.....	40
Activity of sscFv analogues in human plasma .....	41
Stability of the maleimide bridge against reducing agents.....	41
PEGylation of the sscFv via lysines .....	41
Activity of different PEG-sscFv species .....	41
Cell binding assay with fluorescein-sscFv .....	42
One-step ELISAs with HRP-sscFv.....	42
Two-step ELISA with on-plate formation of HRP-sscFv .....	42

Simulation of EPR spectra .....	43
Data fitting process.....	43
Preparation of cartoons .....	43
<b>Synthesis.....</b>	<b>43</b>
Dibromomaleimide-N-biotin.....	43
3,4-Dibromo-2,5-dioxo-2,5-dihydro-pyrrole-1-carboxylic acid methyl ester .....	44
Dibromomaleimide-N-PROXYL spin label .....	44
Dithiophenolmaleimide-N-PROXYL spin label (TPMP) .....	45
Dibromomaleimide-N-methyl-PROXYL spin label .....	46
Dithiophenolmaleimide-N-methyl-PROXYL spin label (TPM <sub>C</sub> P).....	46
<b>References .....</b>	<b>47</b>

# Supplementary Figures

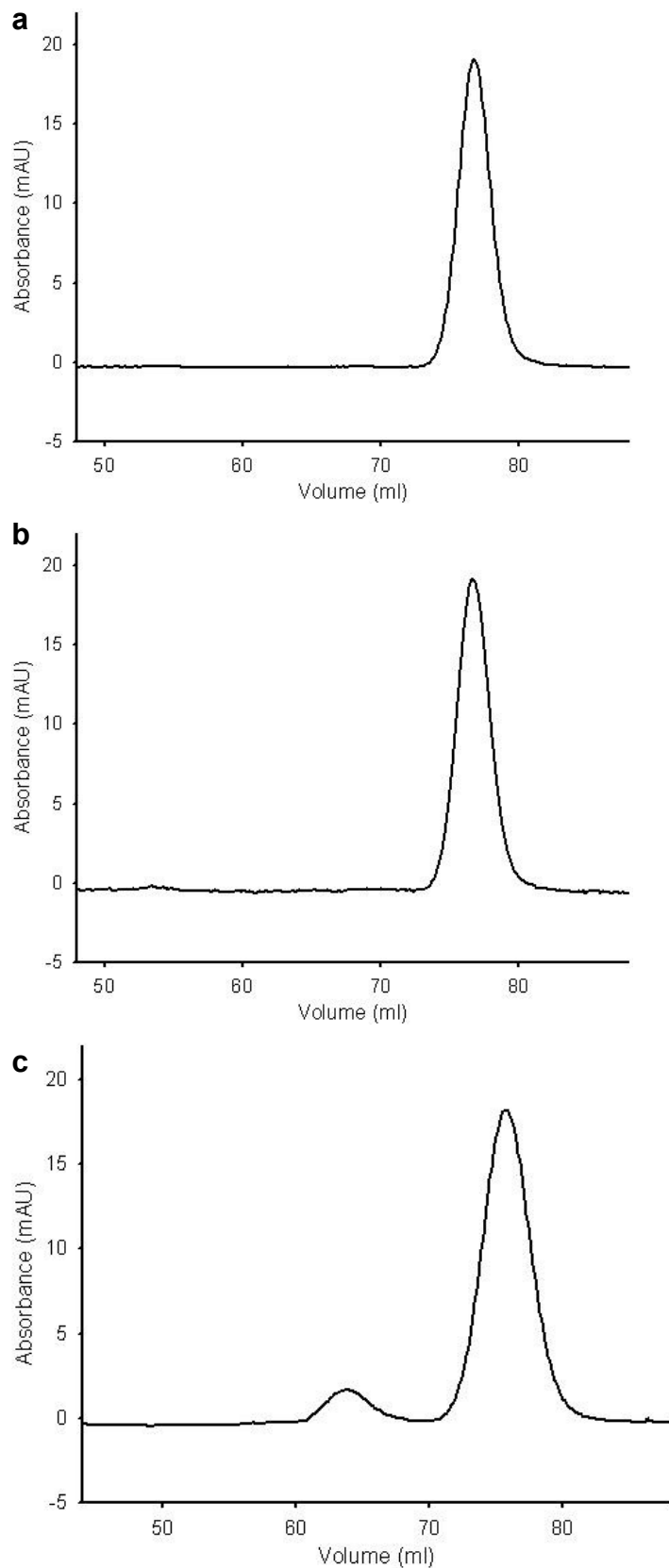
## Supplementary Figure S1: Purification of the sscFv



**a)** Preparative size-exclusion chromatography profile (Superdex 75): The concentrated IMAC fraction containing the sscFv resolves in two fractions.

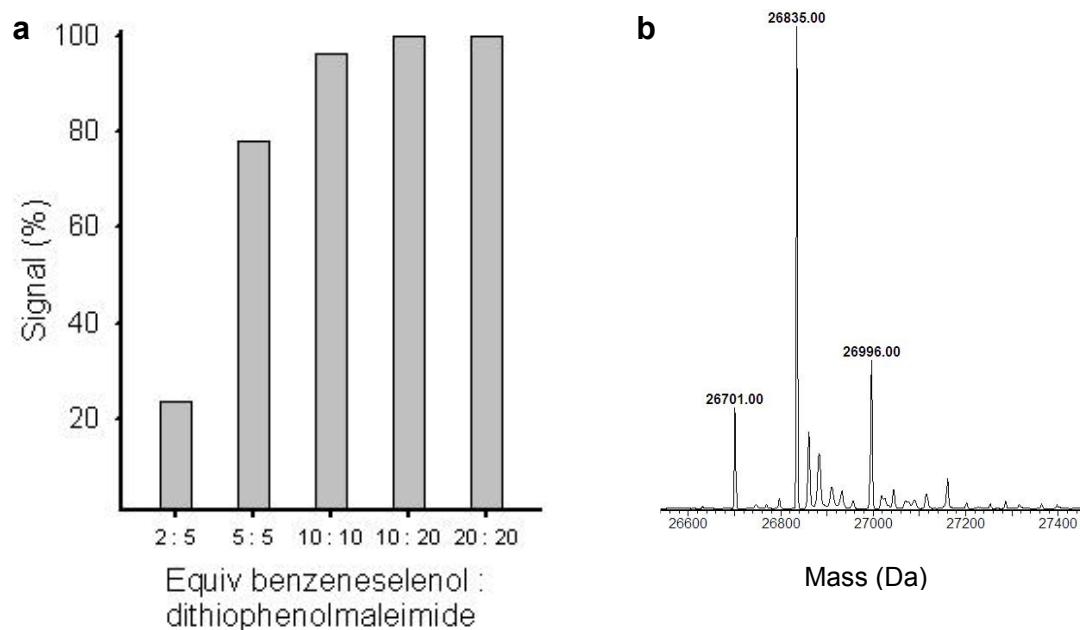
- b)** Analytical size-exclusion chromatography profile of peak 1 (Superdex 75): MW standard (grey, kDa) = 670, 158, 44, 17, 1.35. Calculated MW for peak 1 = 39.5 kDa.
- c)** Analytical size-exclusion chromatography profile of peak 2 (Superdex 75): MW standard (grey, kDa) = 670, 158, 44, 17, 1.35. Calculated MW for peak 2 = 18.2 kDa.
- d)** PAGE of reduced and native sscFv and purification fractions: (1 and 4) purified sscFv. (2 and 5) peak 1. (3 and 6) peak 2.
- e)** SDS-PAGE of reduced and non-reduced sscFv and purification fractions (all samples were boiled and loading buffer contains SDS): (1 and 4) purified sscFv. (2 and 5) peak 1. (3 and 6) peak 2.

## Supplementary Figure S2: FPLC analysis of variously bridged sscFv



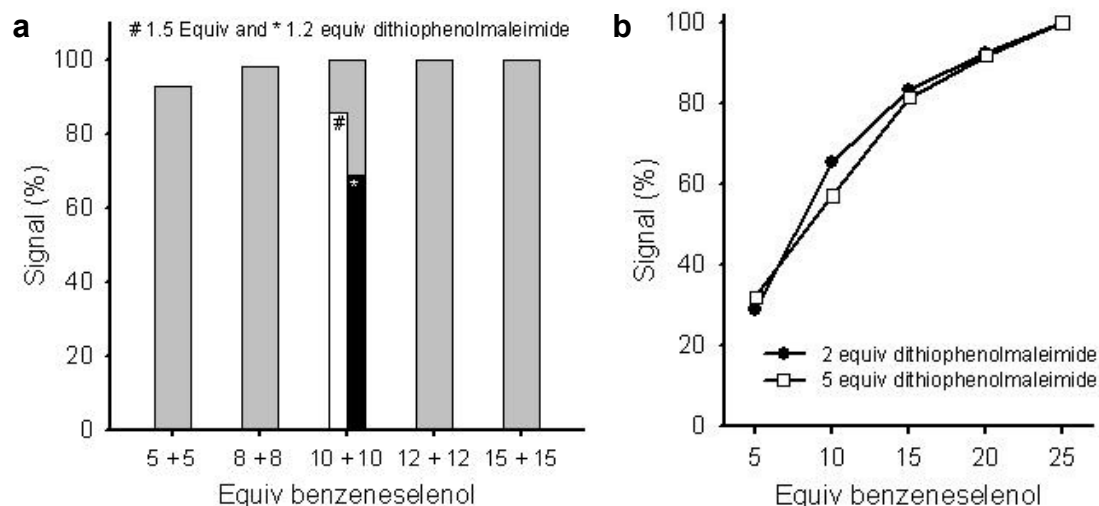
- a)** FPLC analysis of processed sscFv.  
**b)** FPLC analysis of *in situ* bridged sscFv.  
**c)** FPLC analysis of sequentially bridged sscFv.

### Supplementary Figure S3: *In situ* bridging of the sscFv



- a)** Testing of the *in situ* protocol: to the CEA-specific sscFv were added various amounts of dithiophenolmaleimide followed by various amounts of benzeneselenol to yield the following combinations (bridging agent : reducing agent): 5 : 2, 5 : 5, 10 : 10, 20 : 10 and 20 : 20. The reactions were kept at ambient temperature for 1 h and were analysed by LC-MS. The signal refers to the relative abundance of bridged sscFv.
- b)** Deconvoluted LC-MS spectrum of *in situ* bridged sscFv.

### Supplementary Figure S4: Optimization of the *in situ* protocol

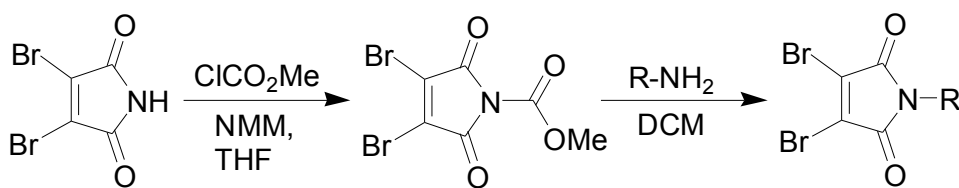


**a)** *In situ* bridging with two portions of benzeneselenol: to the sscFv were added 2 equiv of dithiophenolmaleimide. A variable amount of benzeneselenol was added for 15 min at ambient temperature followed by an identical amount of benzeneselenol for additional 15 min. The samples were analysed by LC-MS. The best combination of reducing agent was also tested for 1.2 and 1.5 equiv of dithiophenolmaleimide. The signal refers to the relative abundance of bridged sscFv.

**b)** *In situ* bridging with a single addition of benzeneselenol: to the sscFv were added 2 or 5 equiv of dithiophenolmaleimide followed by various amounts of benzeneselenol. The reaction was maintained at ambient temperature for 20 min and analysed by LC-MS. The signal refers to the relative abundance of bridged sscFv.

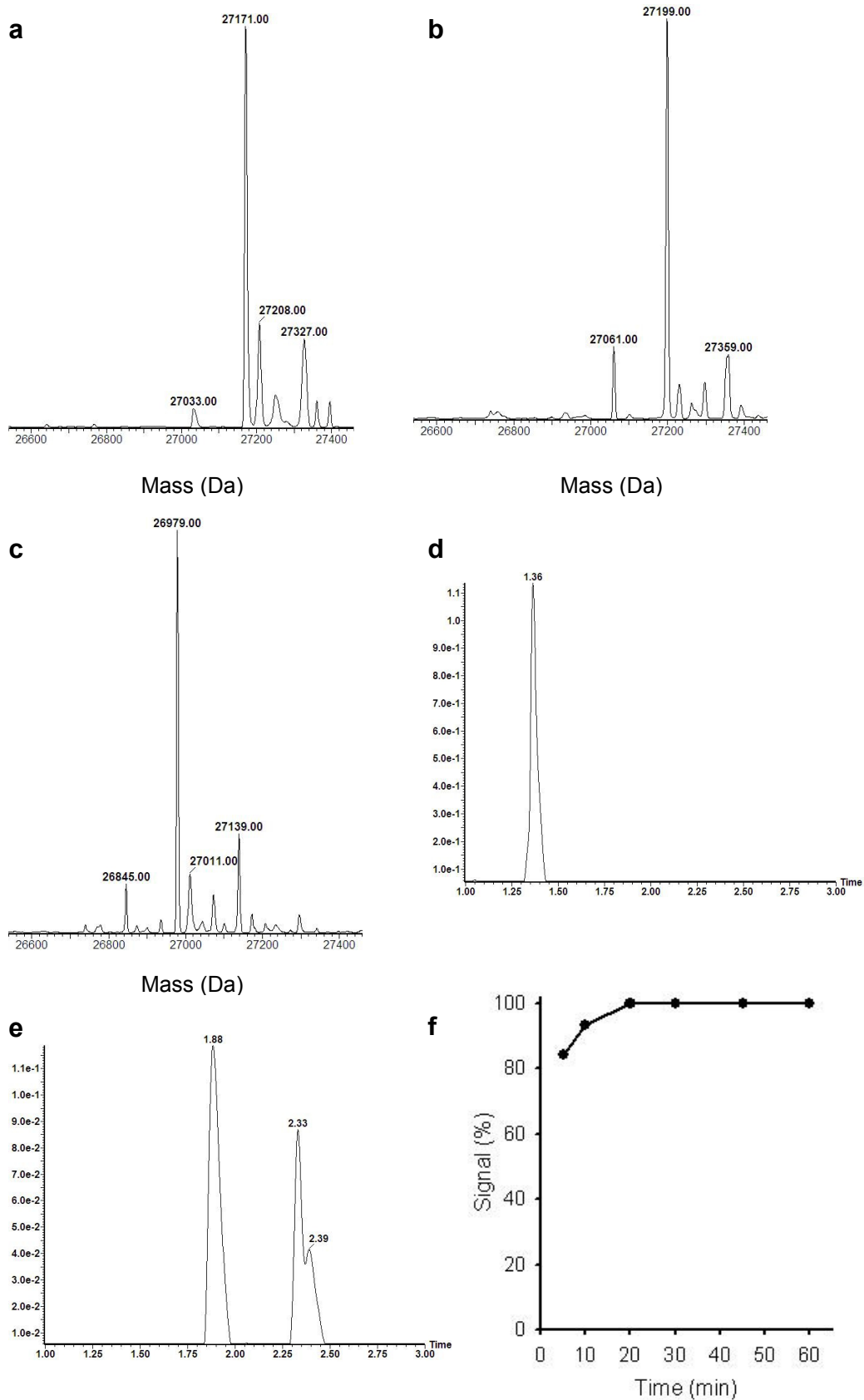


**Supplementary Figure S5: Mild chemical synthesis of N-functionalized maleimides**



Abbreviations: NMM = N-methyl morpholine; THF = tetrahydrofuran; DCM = dichloromethane; R = functional group. See Supplementary Methods for conditions and yield.

## Supplementary Figure S6: Functionalisation of the sscFv



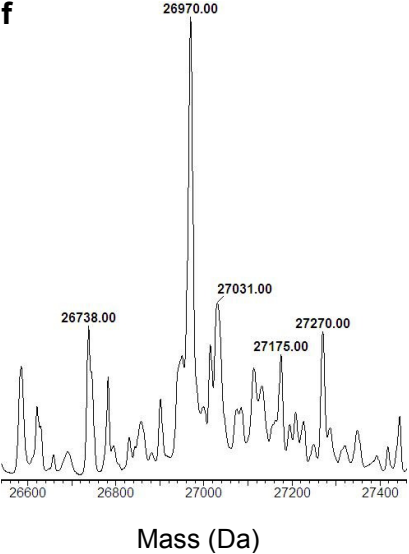
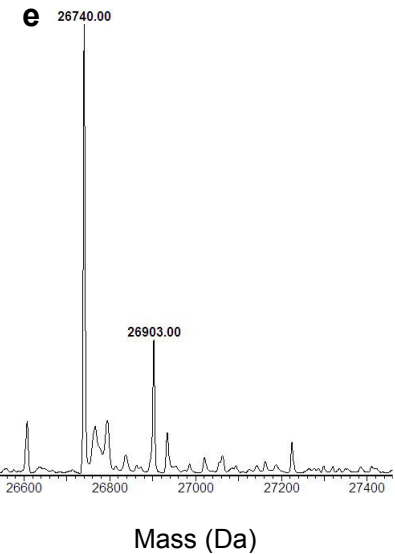
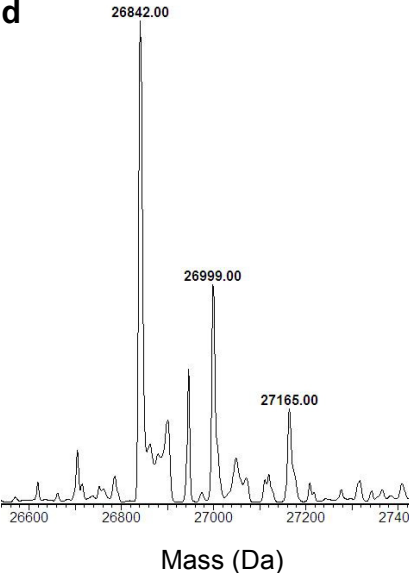
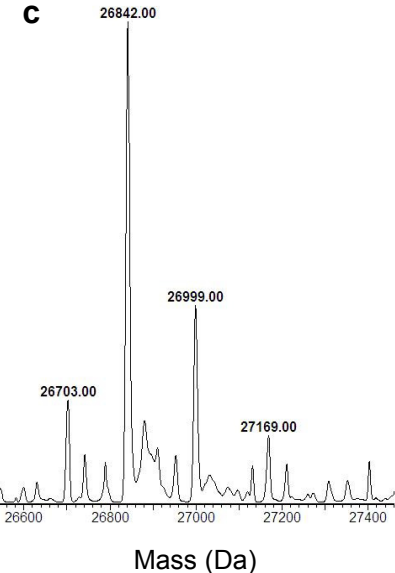
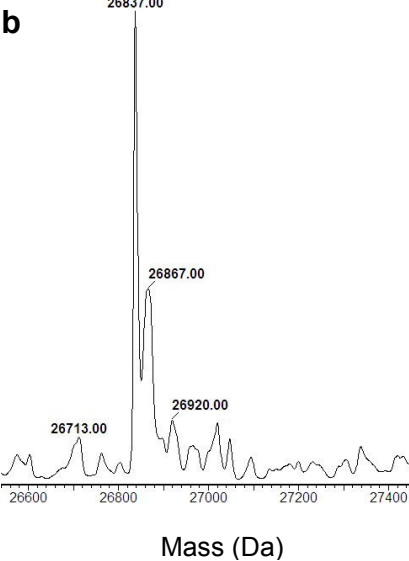
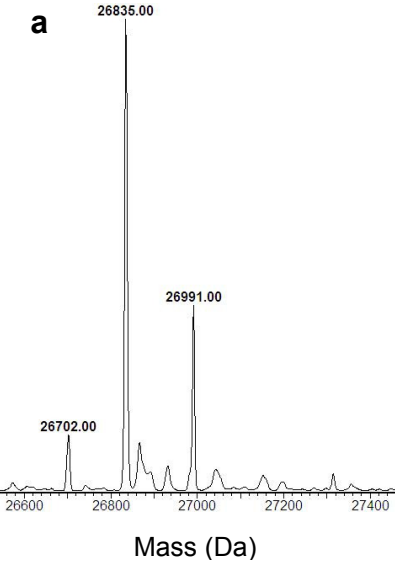
**a)** Deconvoluted LC-MS spectrum of fluorescein-sscFv (requires 27,171 Da).  
**b)** Deconvoluted LC-MS spectrum of biotin-sscFv (requires 27,197 Da).  
**c)** Deconvoluted LC-MS spectrum of spin labeled sscFv (requires 26,978 Da).

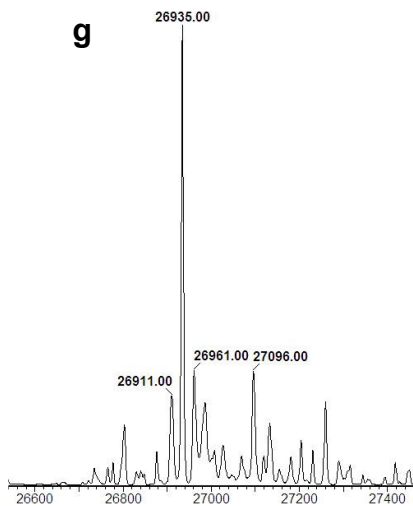
**d)** LC elution profile of the sscFv.

**e)** LC elution profile of the reaction mixture for *in situ* PEGylation of the sscFv. The main peak (1.88 min) corresponds to the PEGylated antibody fragment; additional peaks (2.33 and 2.39) correspond to the PEGylation reagent.

**f)** Timed LC-MS data of the *in situ* PEGylation reaction of the sscFv: To the sscFv were added 15 equiv of N-PEG5000-dithiophenolmaleimide followed by addition of 15 equiv of benzeneselenol. The reaction was maintained for 60 min at ambient temperature and aliquots withdrawn at various time points for analysis by LC-MS. The reaction was monitored by the disappearance of the LC signal of the unmodified protein. The signal refers to the relative abundance of PEG-sscFv.

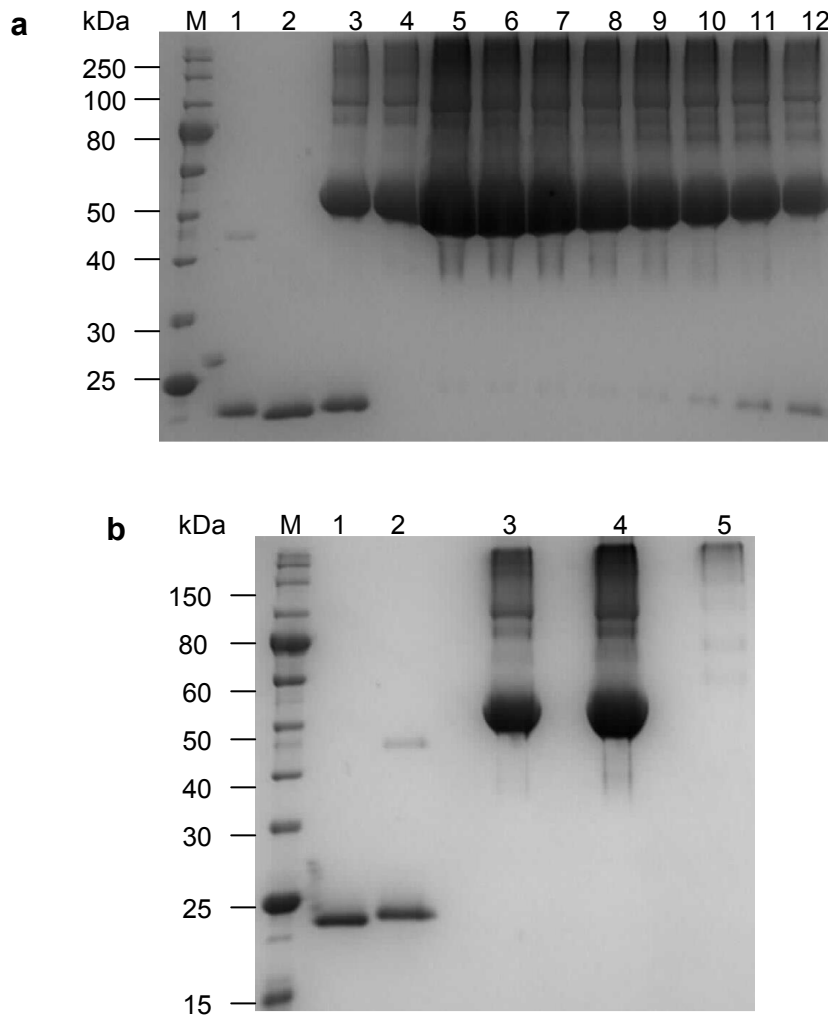
Supplementary Figure S7: Stability of sscFv analogues in human plasma





- a)** Deconvoluted LC-MS spectrum of bridged sscFv isolated after 1 h from human plasma.
- b)** Deconvoluted LC-MS spectrum of bridged sscFv isolated after 24 h from human plasma.
- c)** Deconvoluted LC-MS spectrum of bridged sscFv isolated after 3 d from human plasma.
- d)** Deconvoluted LC-MS spectrum of bridged sscFv isolated after 7 d from human plasma. The increase in molecular weight is possibly due to the presence of antibody fragment with a hydrolysed maleimide bridge (+18 Da for a molecule of water) which is not distinguished from the non-hydrolysed material by the deconvolution software.
- e)** Deconvoluted LC-MS spectrum of unmodified sscFv isolated as a control after 7 d from human plasma.
- f)** Deconvoluted LC-MS spectrum of alkylated sscFv isolated as a control after 7 d from human plasma (requires 26936 Da). The increased mass of the main peak corresponds to a species with both maleimide molecules hydrolysed (+38 Da, requires 26972 Da).
- g)** Deconvoluted LC-MS spectrum of alkylated sscFv.

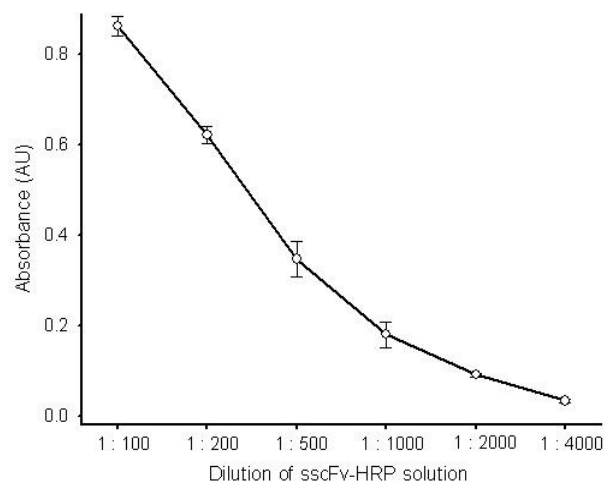
## Supplementary Figure S8: Preparation and purification of HRP-sscFv conjugate



**a**) Synthesis of the HRP-sscFv conjugate: (1) Biotin-sscFv. (2) Unmodified sscFv. (3) Mix of unmodified sscFv and the HRP-Strep conjugate. (4) HRP-Strep conjugate. (5) Mix of 15  $\mu$ l of biotin-sscFv (20  $\mu$ M) with 15  $\mu$ l, (6) 12  $\mu$ l, (7) 10  $\mu$ l, (8) 8  $\mu$ l, (9) 6  $\mu$ l, (10) 4  $\mu$ l, (11) 2  $\mu$ l and (12) 1  $\mu$ l of HRP-Strep solution (1.25 mg ml<sup>-1</sup>).

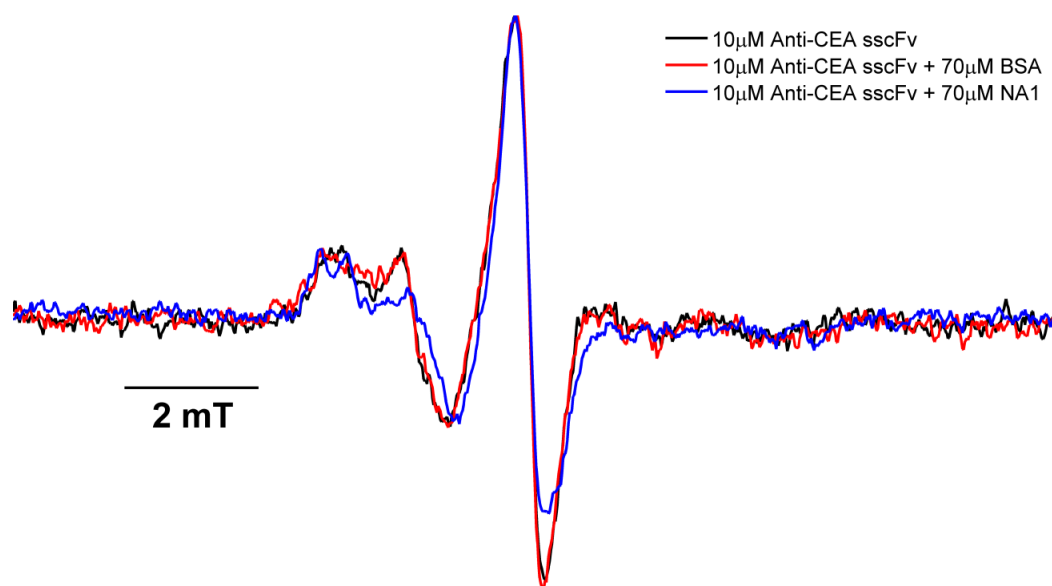
**b**) Purification of the HRP-sscFv conjugate: (1) Unmodified sscFv. (2) Biotin-sscFv. (3) HRP-Strep conjugate. (4) Mix of the biotin-sscFv with a 3x excess (by mass) of HRP-Strep. (5) Purified HRP-sscFv.

### Supplementary Figure S9: Activity of the HRP-sscFv conjugate



One-step ELISA with the HRP-sscFv conjugate: an ELISA plate was coated with full length human CEA ( $1 \mu\text{g ml}^{-1}$ ) and treated with various dilutions of an  $\text{OD}_{280} = 0.4$  solution of purified HRP-sscFv conjugate to determine the activity of the material. Plate read-out was performed as described.

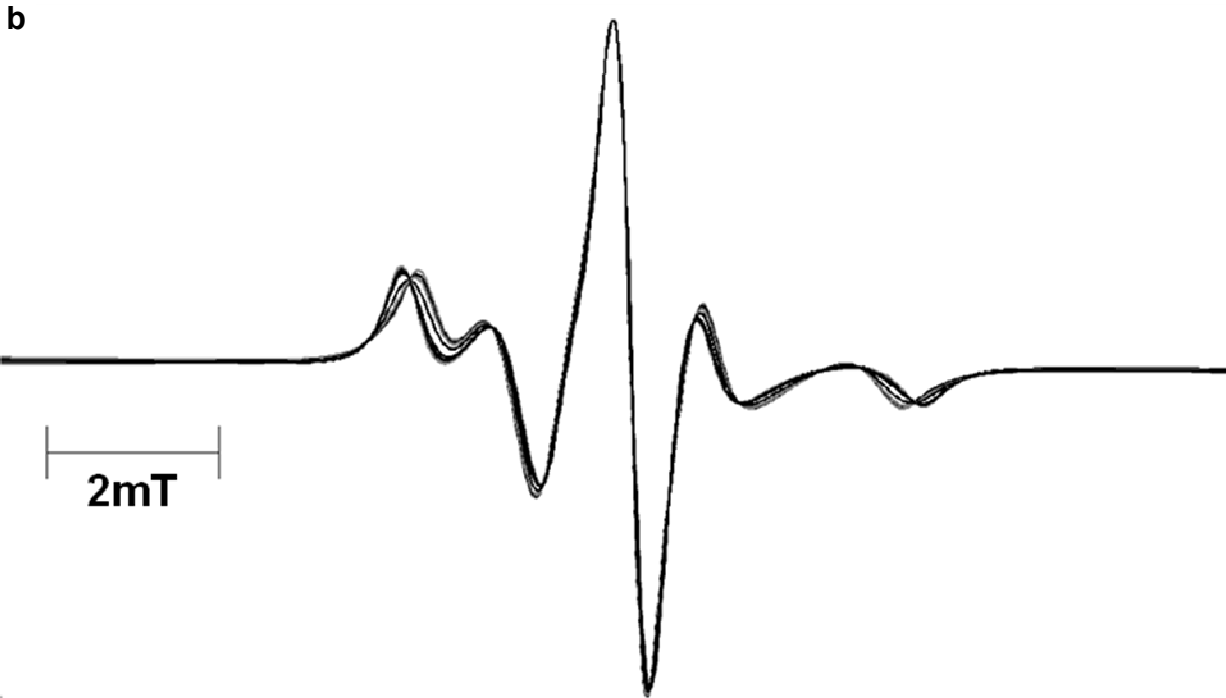
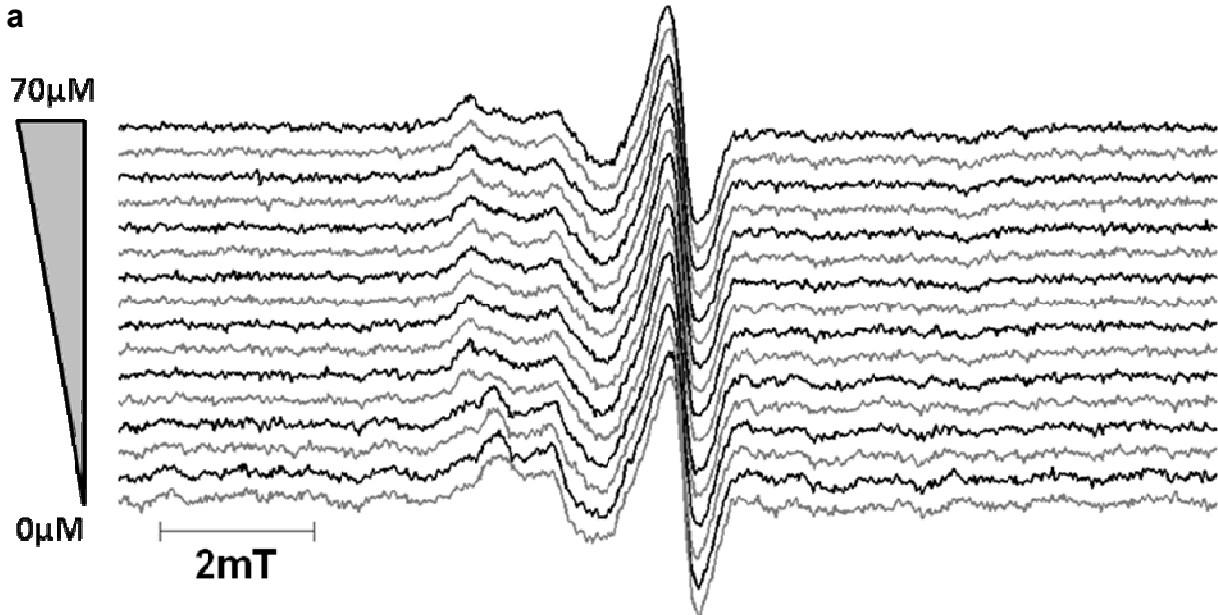
## Supplementary Figure S10: Specificity of the EPR-monitored binding event



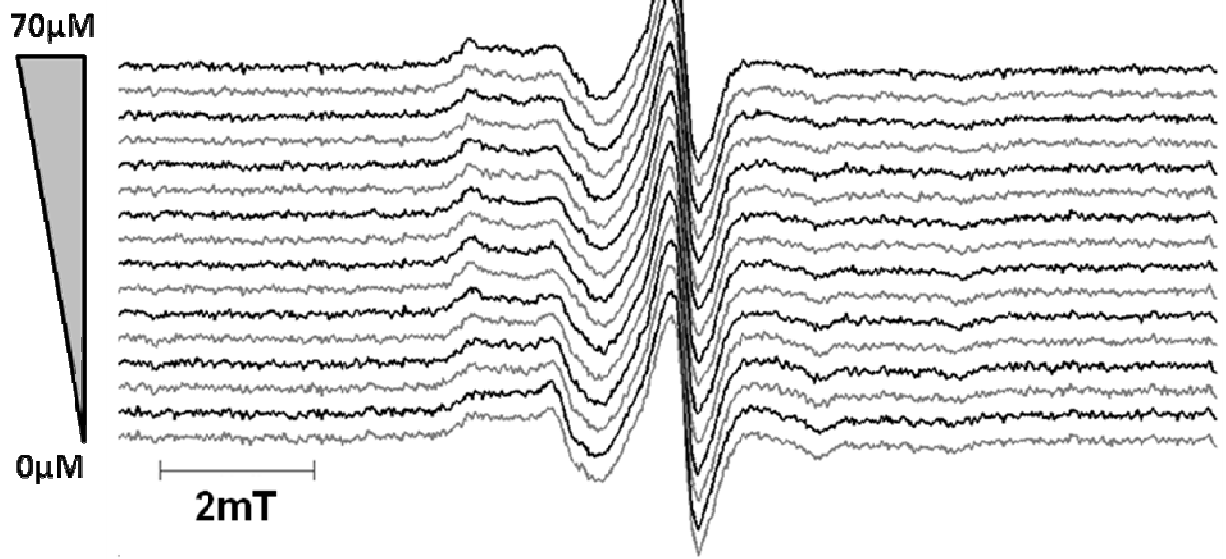
Control of the specificity of the anti-CEA sscFv interaction with NA1: EPR spectra of MP-sscFv (10  $\mu$ M) were recorded as described either in buffer (black line), in the presence of 70  $\mu$ M BSA (red line) or 70  $\mu$ M NA1 (blue line). No non-specific binding was observed.



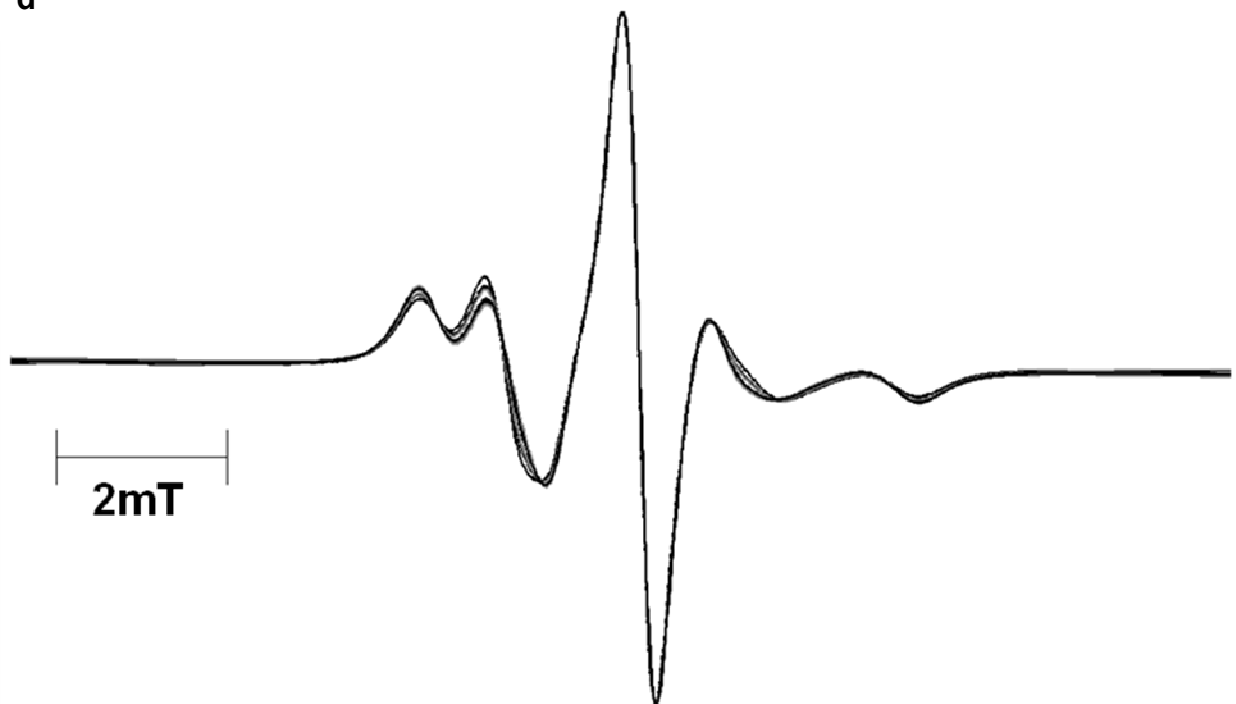
Supplementary Figure S11: 10  $\mu\text{M}$  MP-sscFv and M<sub>C</sub>P-sscFv EPR spectra and simulated spectra



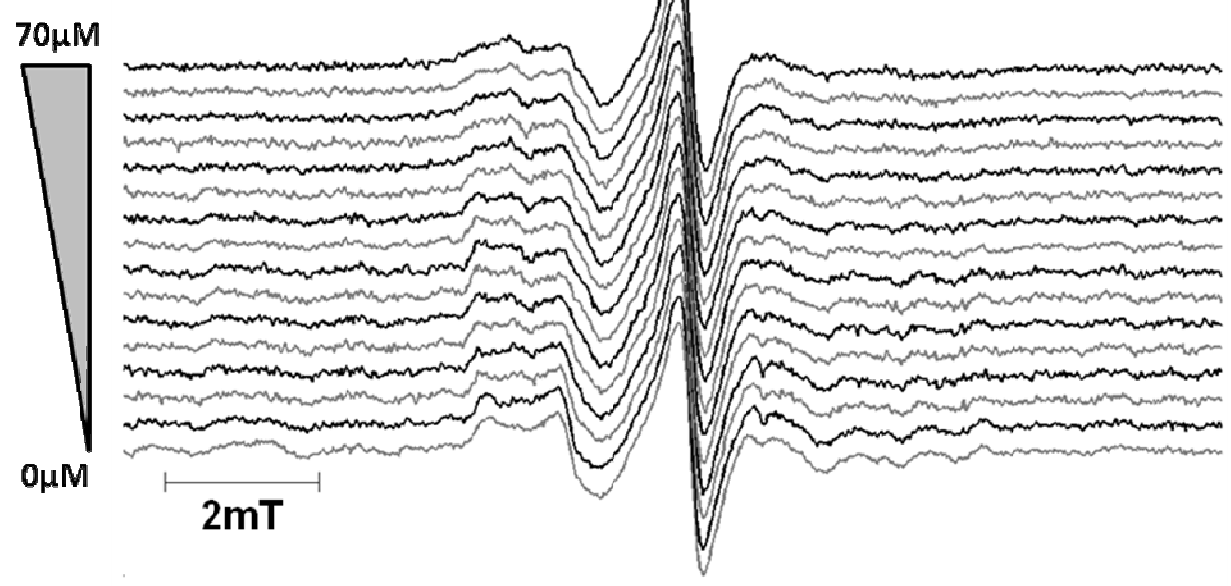
c



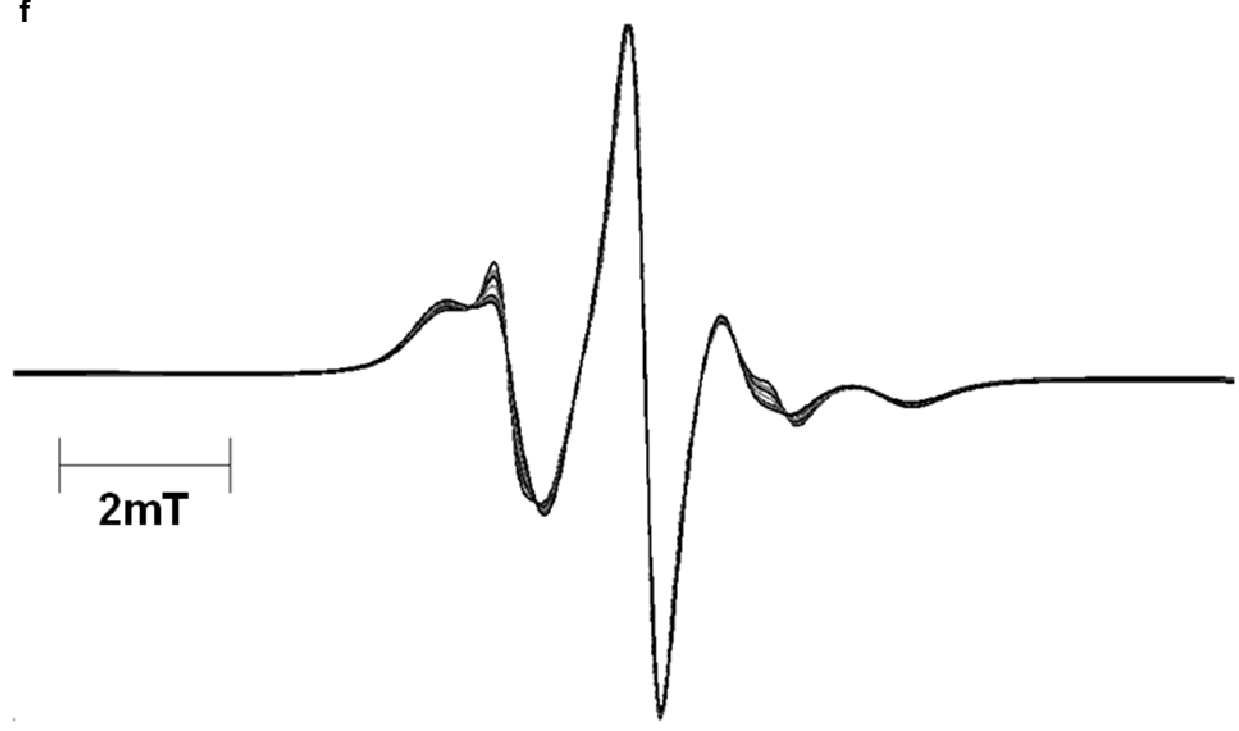
d



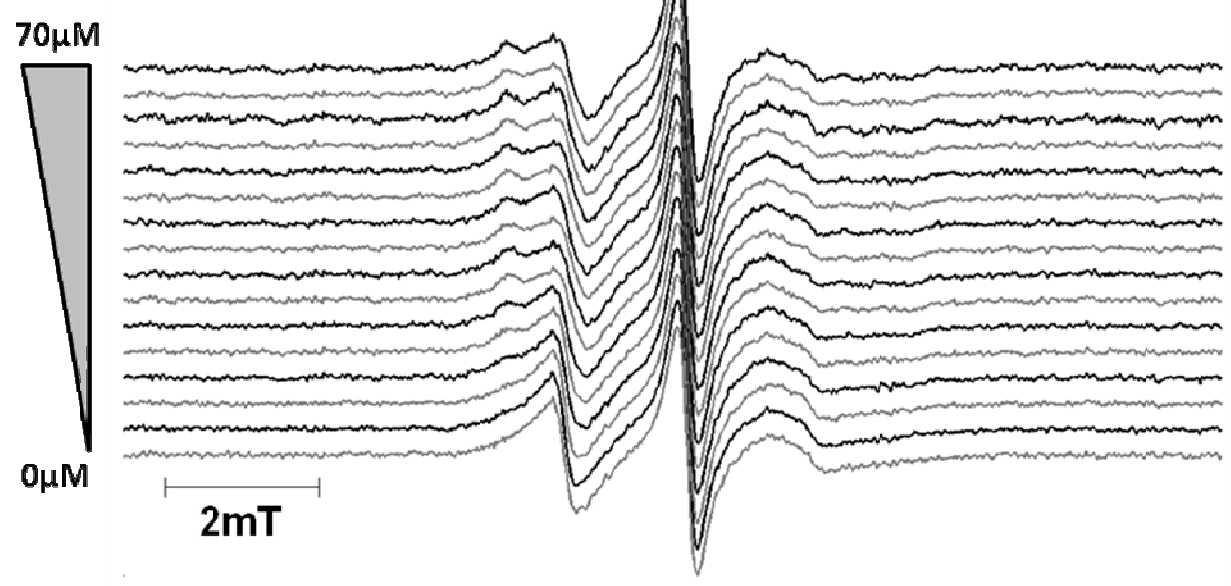
e



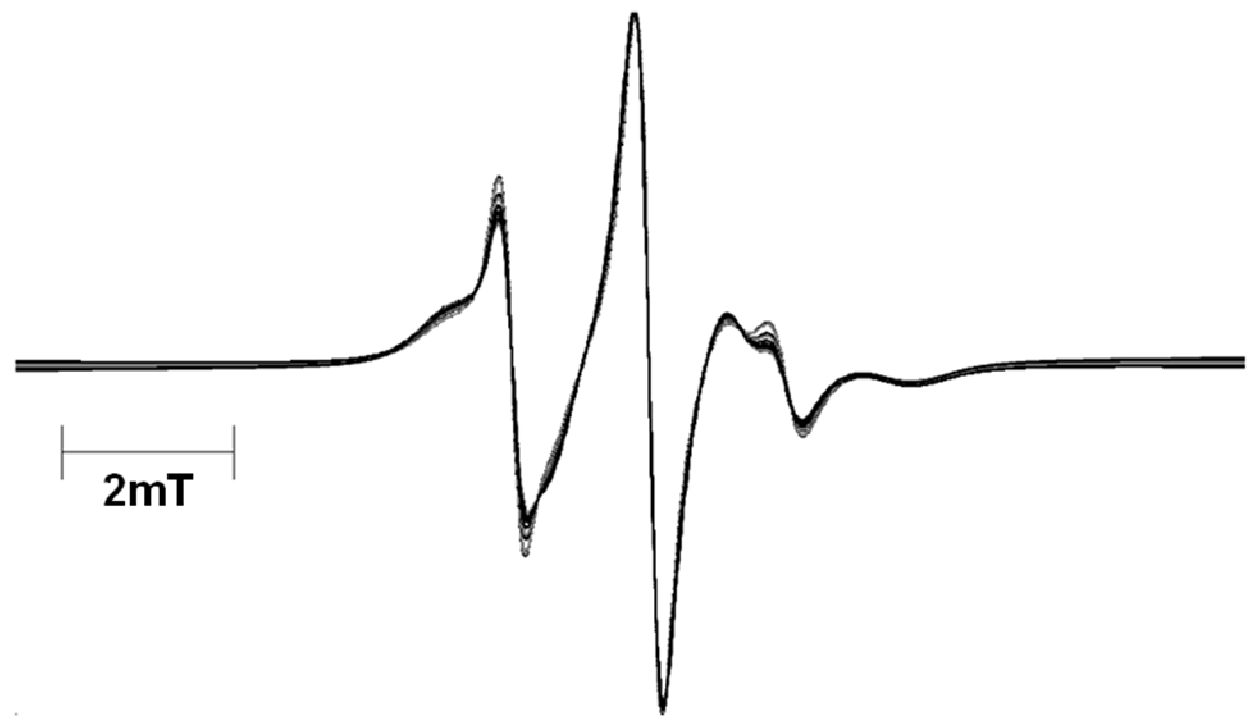
f

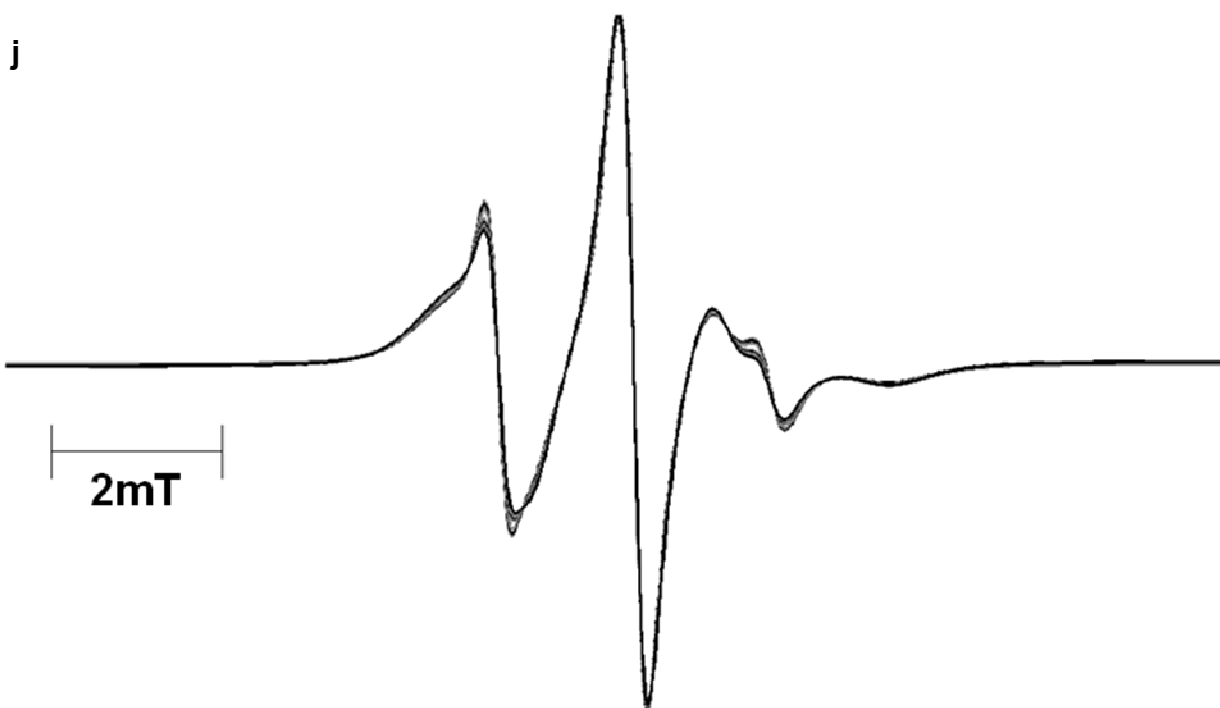
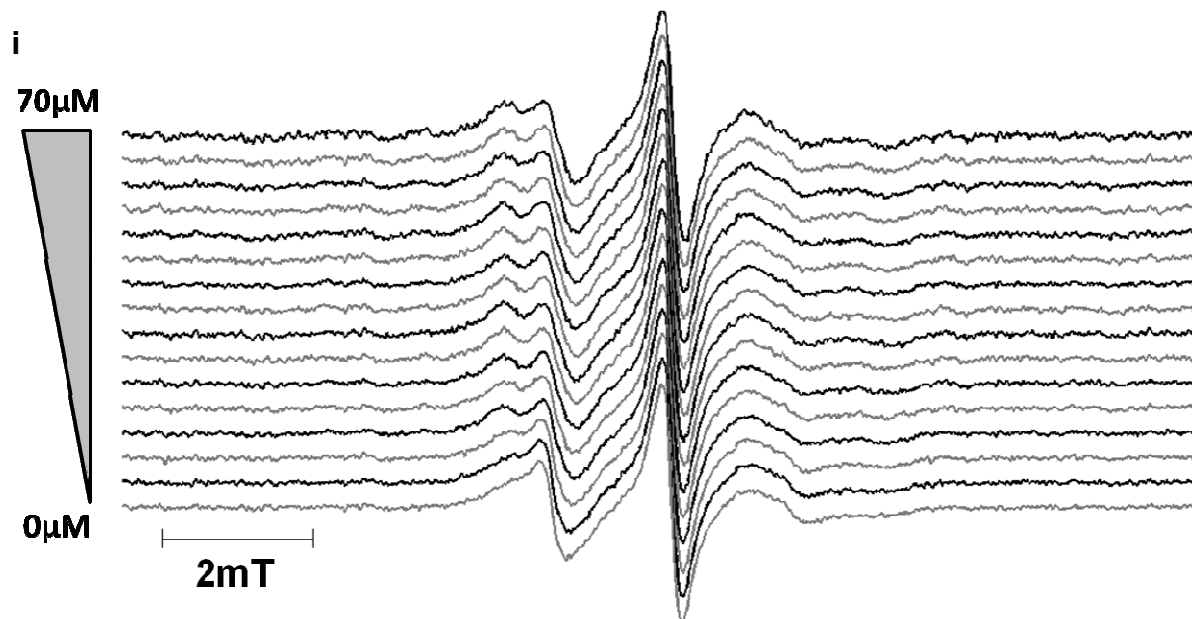


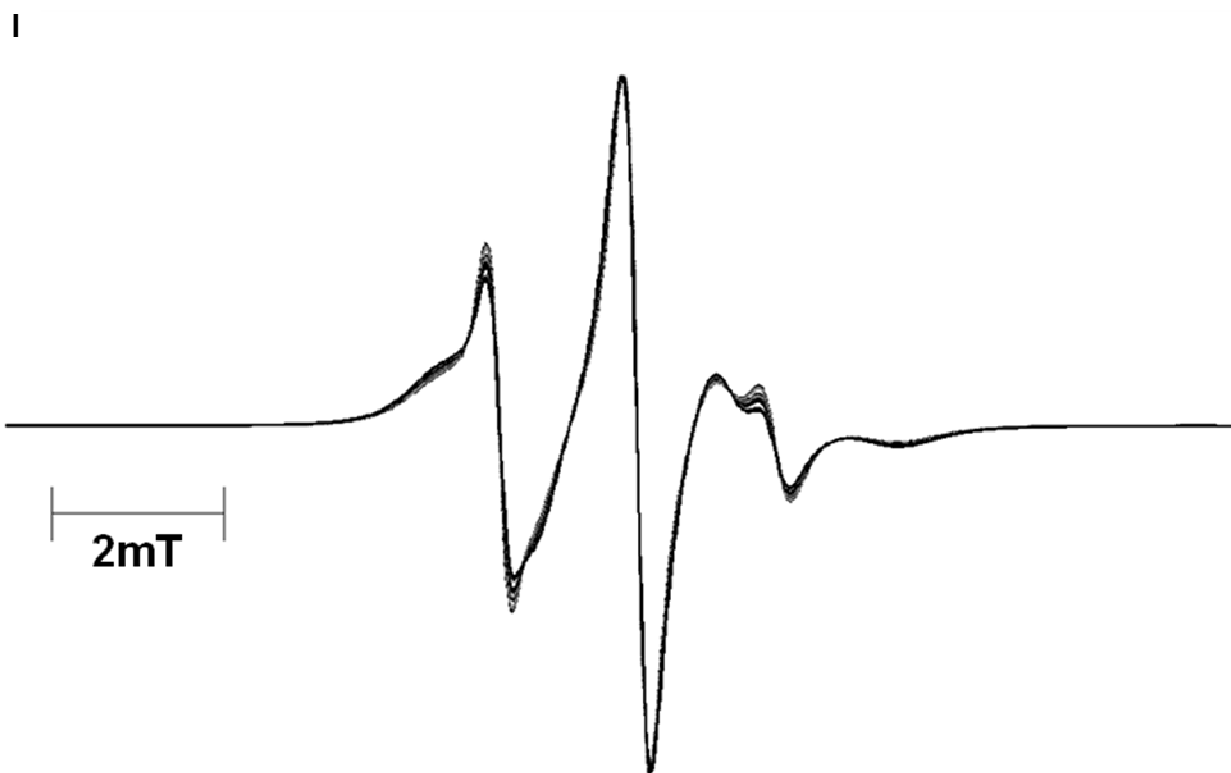
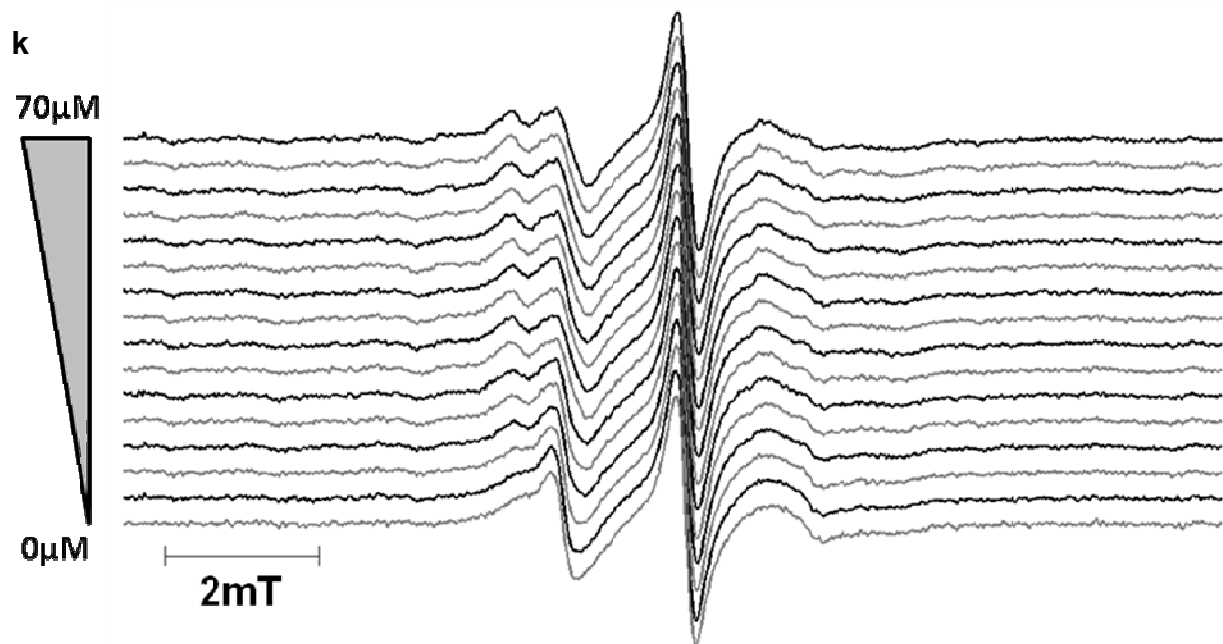
g



h





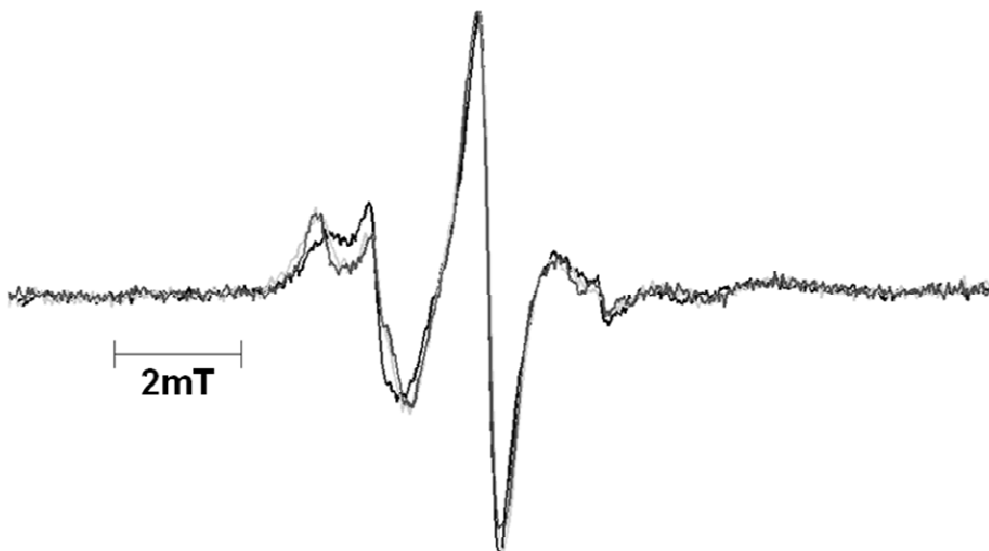


- a) 10  $\mu\text{M}$  MP-sscFv NA1 binding curve ESR spectra. NA1 concentration increases from bottom to top, 0–70  $\mu\text{M}$  in PBS.
- b) Simulated spectra from acquired data a).
- c) Same as a) but in human plasma.
- d) Same as b) but for acquired dataset c).

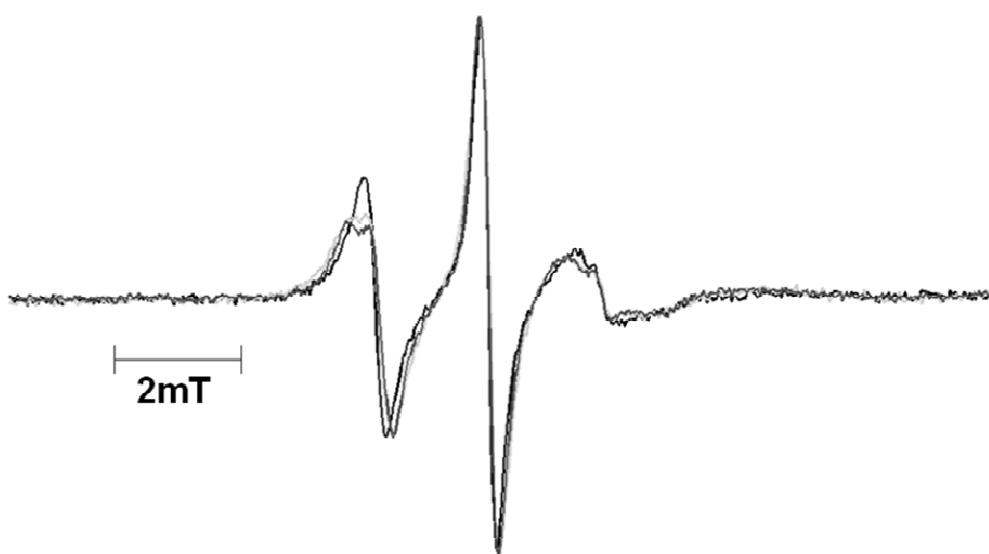
- e)** Same as **a)** but in whole human blood.
- f)** Same as **b)** but for acquired dataset **e)**.
- g)** 10  $\mu\text{M}$   $M_C\text{P-sscFv NA1}$  binding curve ESR spectra. NA1 concentration increases from bottom to top, 0–70  $\mu\text{M}$  in PBS.
- h)** Simulated spectra from acquired data **g)**.
- i)** Same as **g)** but in human plasma.
- j)** Same as **h)** but for acquired dataset **i)**.
- k)** Same as **g)** but in whole human blood.
- l)** Same as **h)** but for acquired dataset **k)**.

Supplementary Figure S12: MP- and M<sub>C</sub>P-sscFv EPR spectra in sucrose

a



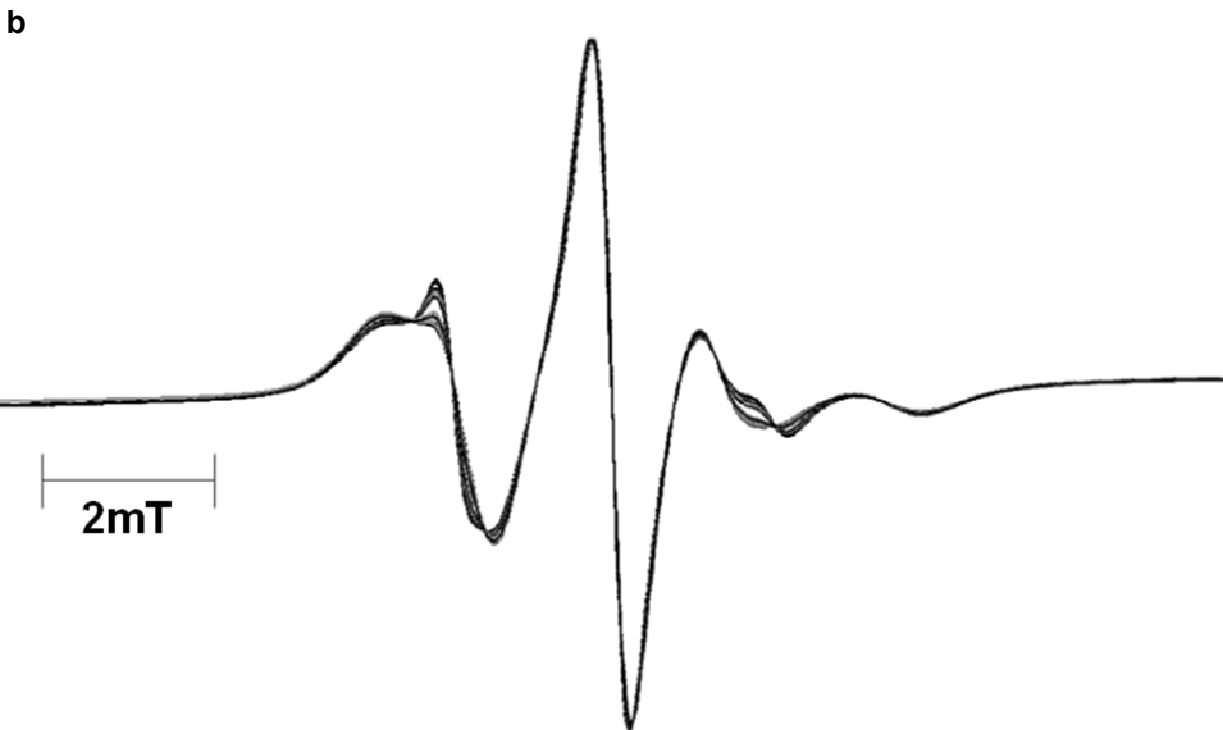
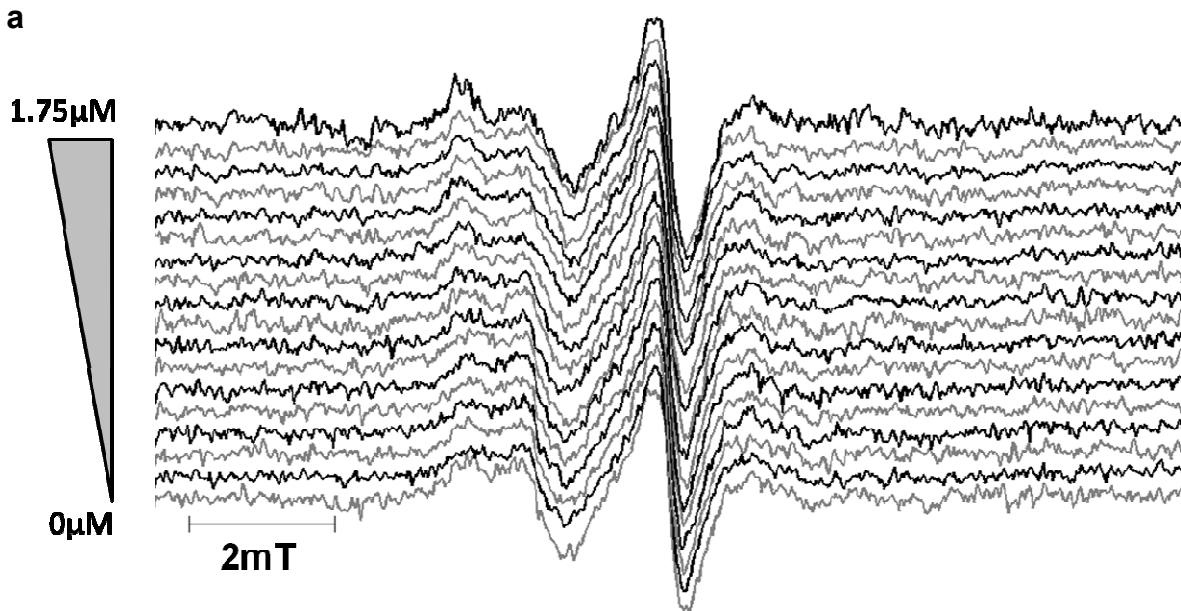
b



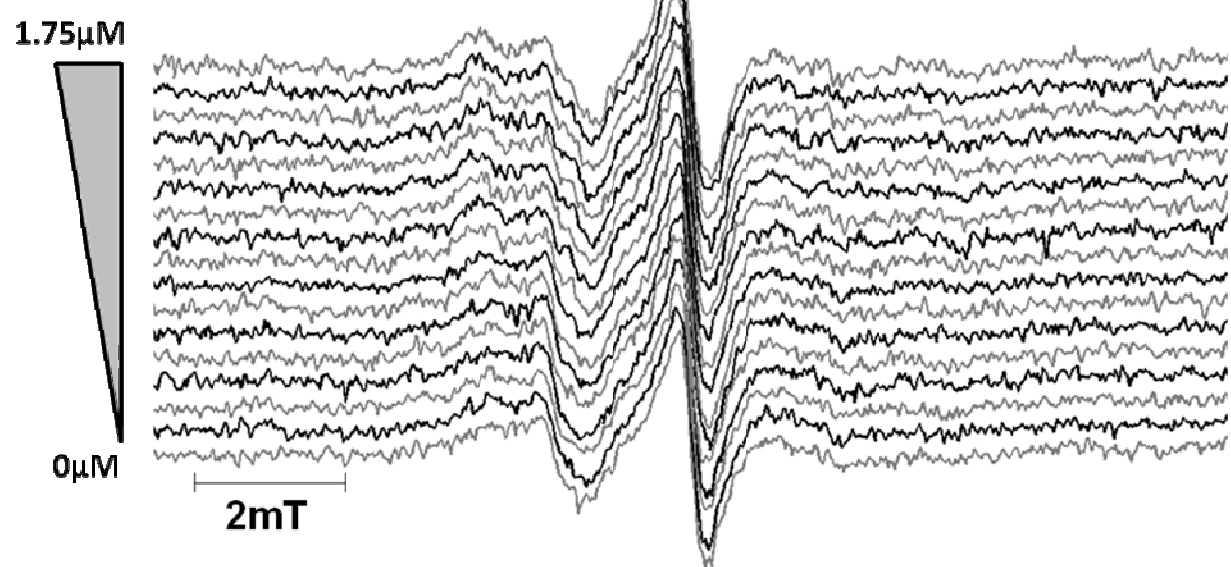
- a) 10  $\mu$ M MP-sscFv (black), NA1 bound (dark grey) and 30% wt/vol sucrose containing (light grey) EPR spectra in PBS.  
b) Same as a) but for M<sub>C</sub>P-sscFv.



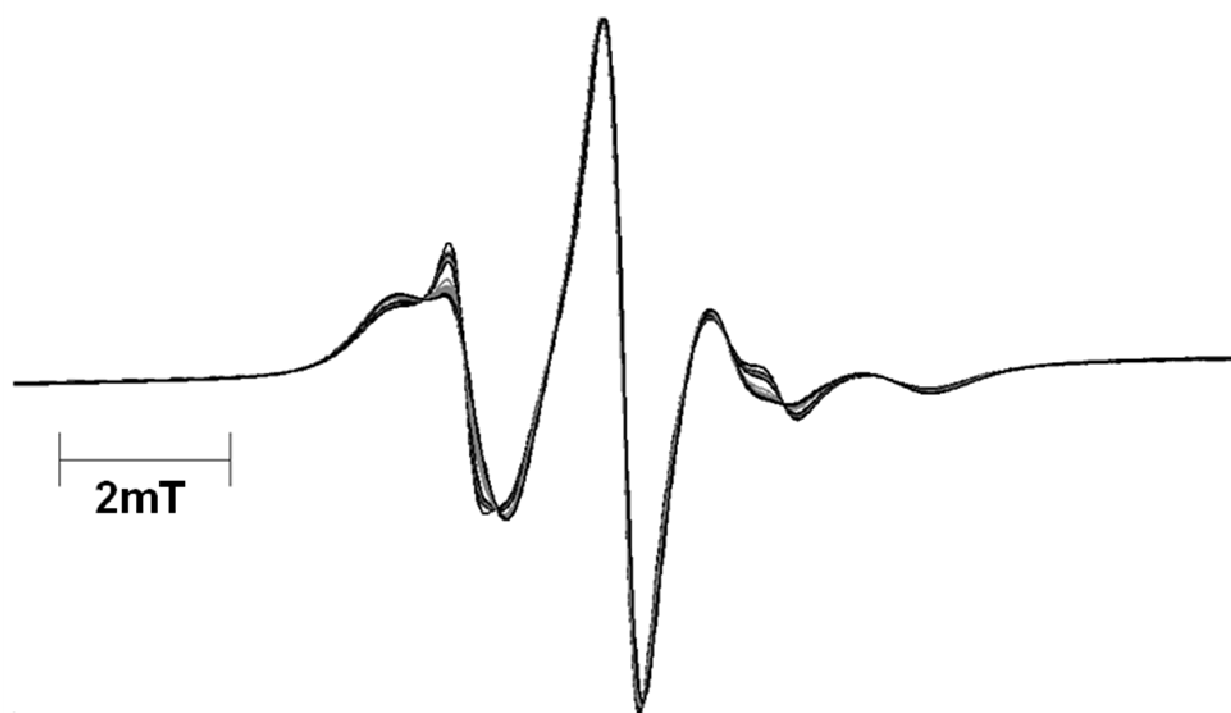
Supplementary Figure S13: 250 nM MP-sscFv and M<sub>C</sub>P-sscFv EPR spectra and simulated spectra



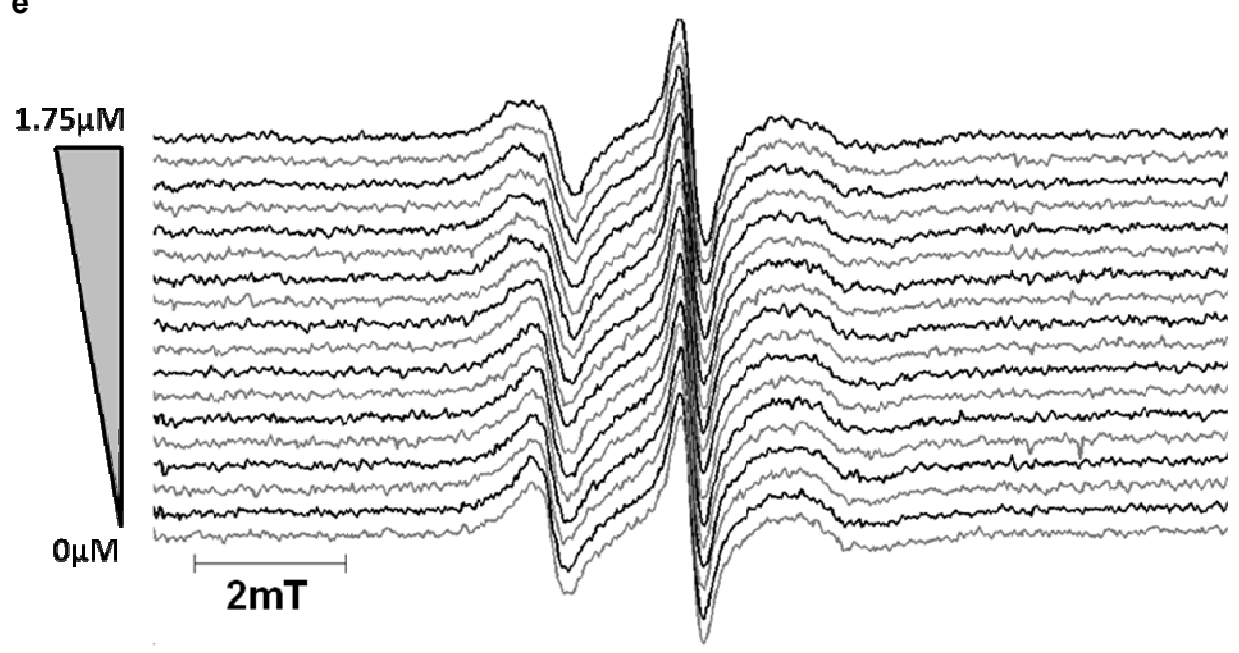
c



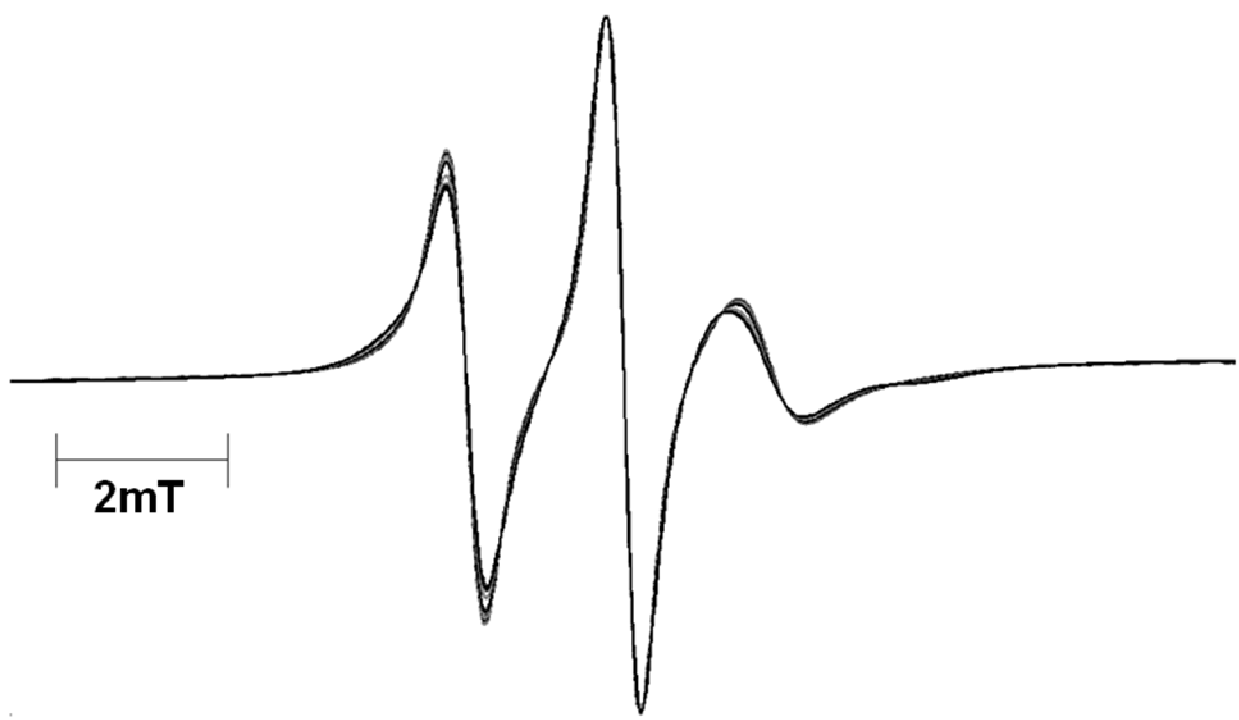
d



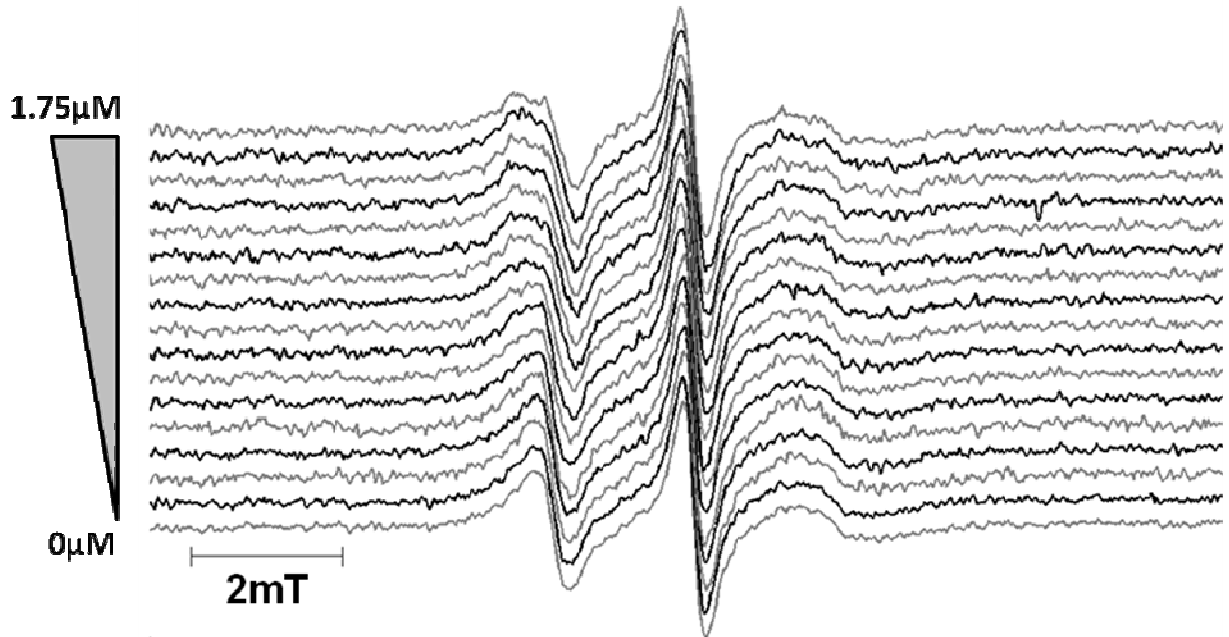
e



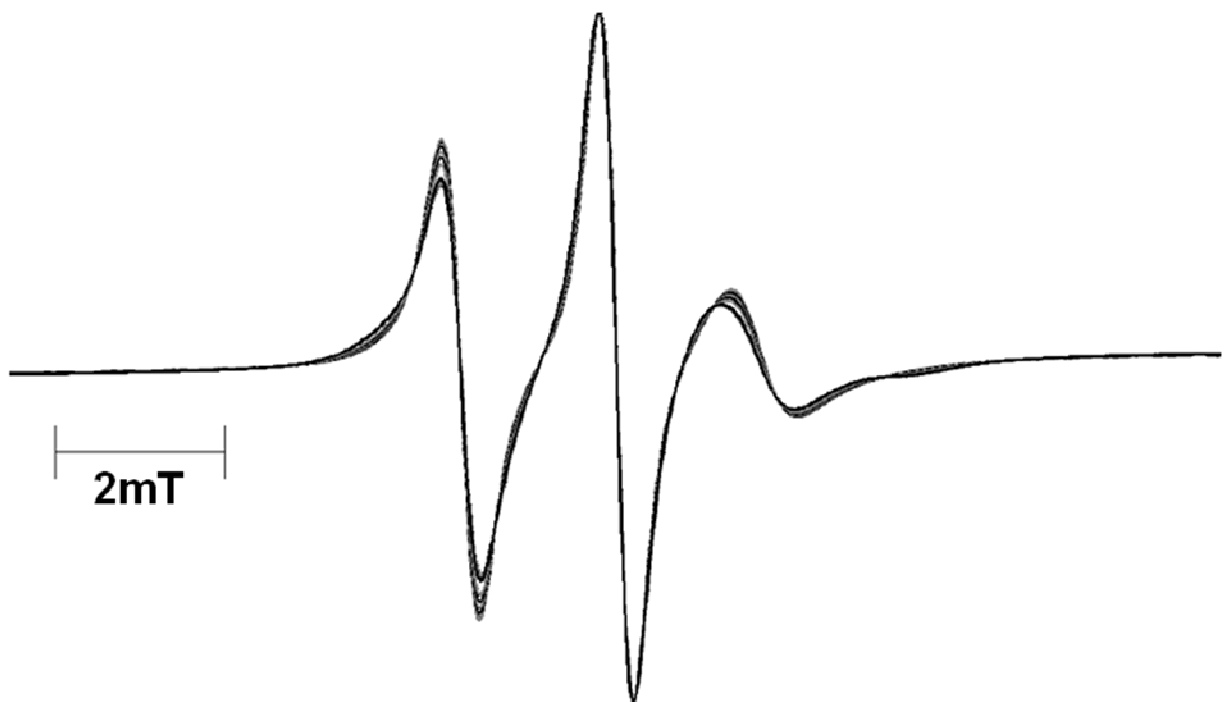
f



g



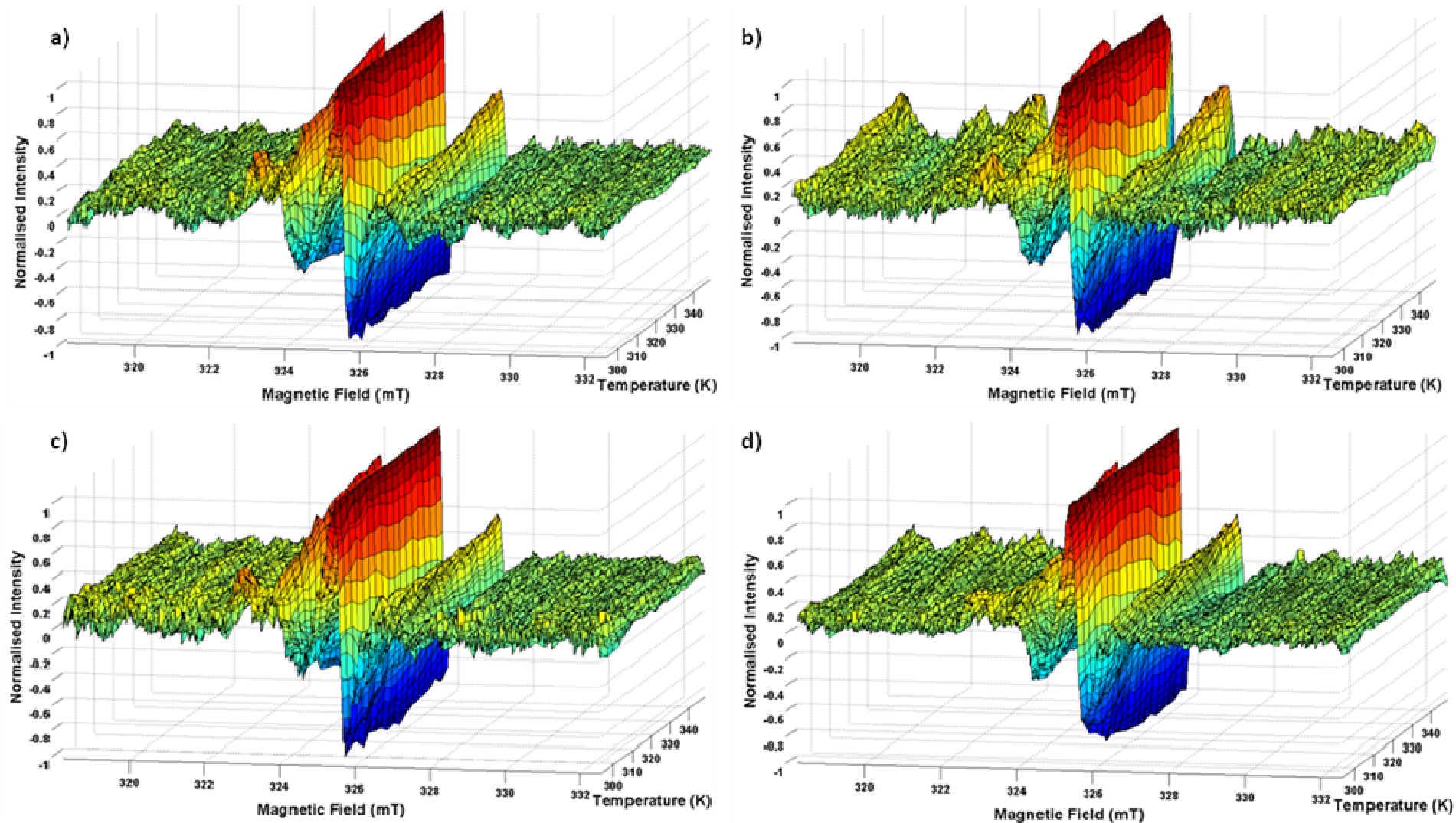
h

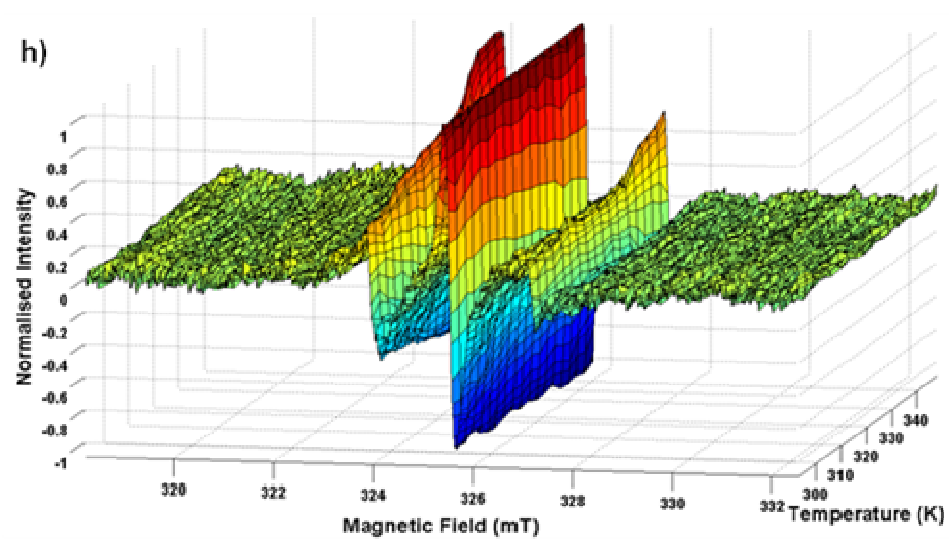
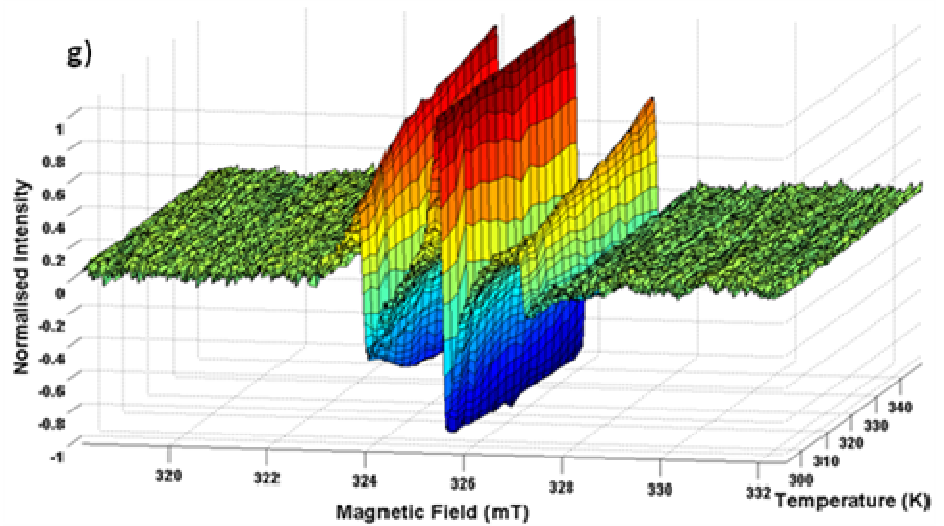
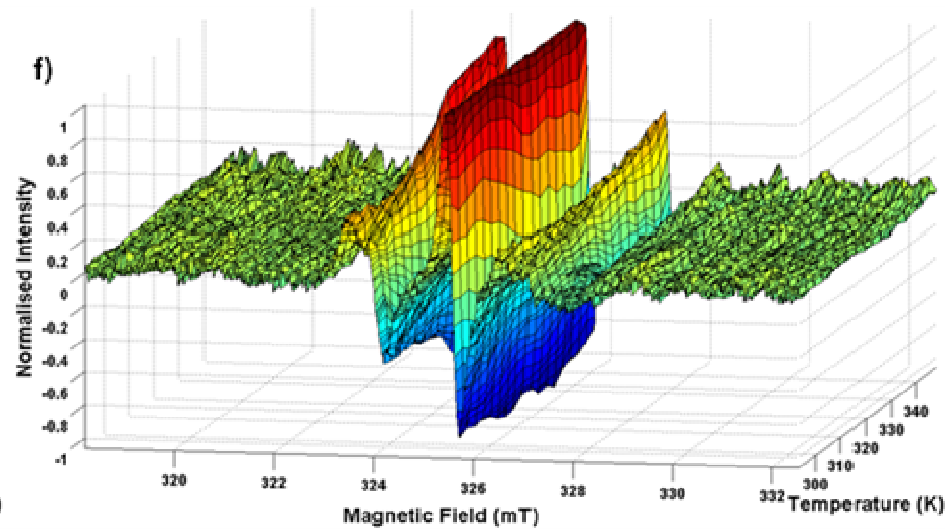
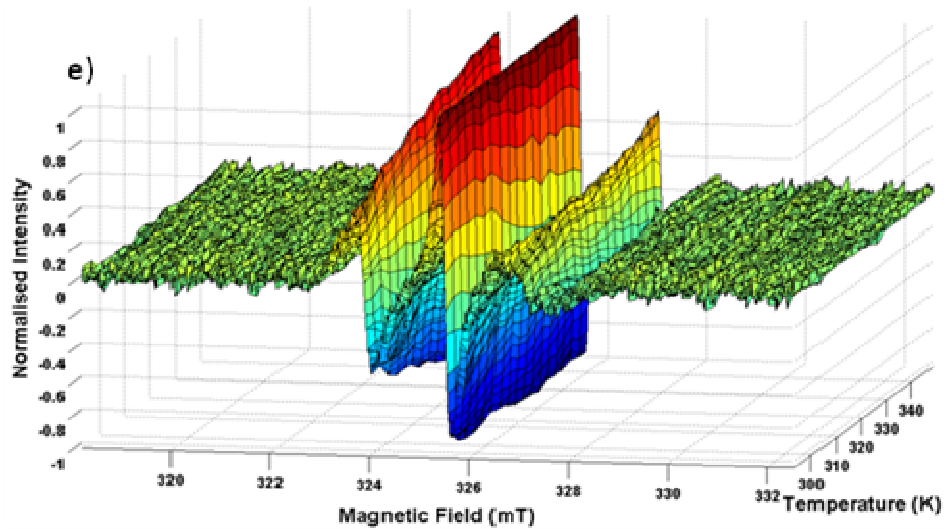


- a) 250 nM MP-sscFv NA1 binding curve ESR spectra. Protein concentration increases from bottom to top, 0–1.75  $\mu\text{M}$  in whole human blood.
- b) Simulated spectra from acquired data a).
- c) Same as a) but with full length CEA.
- d) Same as b) but for acquired dataset c).

- e)** 250 nM M<sub>C</sub>P-sscFv NA1 binding curve ESR spectra. Protein concentration increases from bottom to top, 0–1.75 μM in whole human blood.
- f)** Simulated spectra from acquired data **e**).
- g)** Same as **e**) but with full length CEA.
- h)** Same as **f**) b

Supplementary Figure S14: MP- and M<sub>C</sub>P-sscFv and MP- and M<sub>C</sub>P-sscFv-SM3E with and without NA1 thermal denaturation

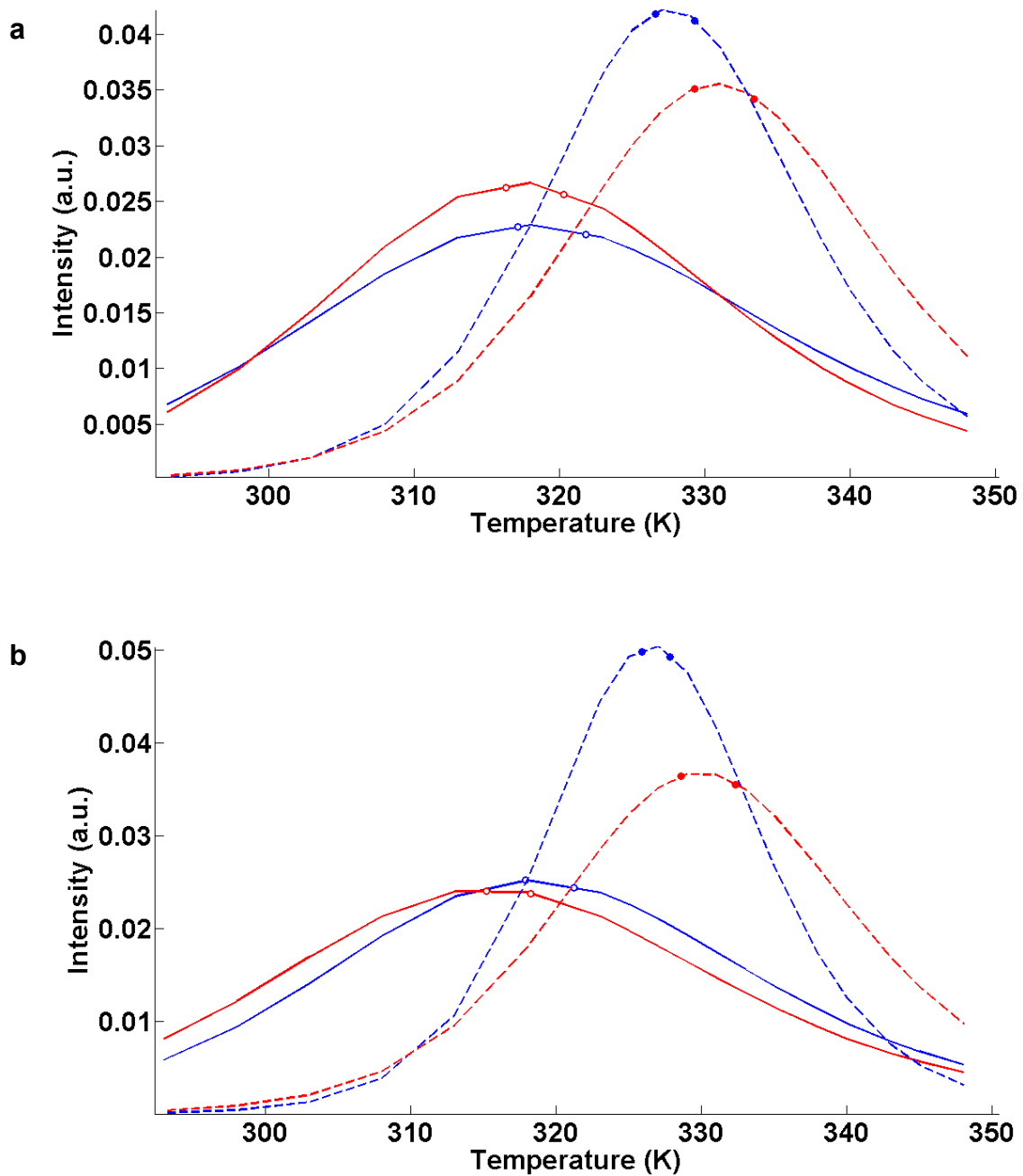




- a)** 10  $\mu\text{M}$  MP-sscFv thermal denaturation profile in PBS.
- b)** Same as **a)** but for MP-sscFv-SM3E.
- c)** Same as **a)** but in the presence of 70  $\mu\text{M}$  NA1.
- d)** Same as **b)** but in the presence of 70  $\mu\text{M}$  NA1.
- e)** 10  $\mu\text{M}$  M<sub>C</sub>P-sscFv thermal denaturation profile in PBS.
- f)** Same as **a)** but for M<sub>C</sub>P-sscFv-SM3E.
- g)** Same as **a)** but in the presence of 70  $\mu\text{M}$  NA1.
- h)** Same as **b)** but in the presence of 70  $\mu\text{M}$  NA1.

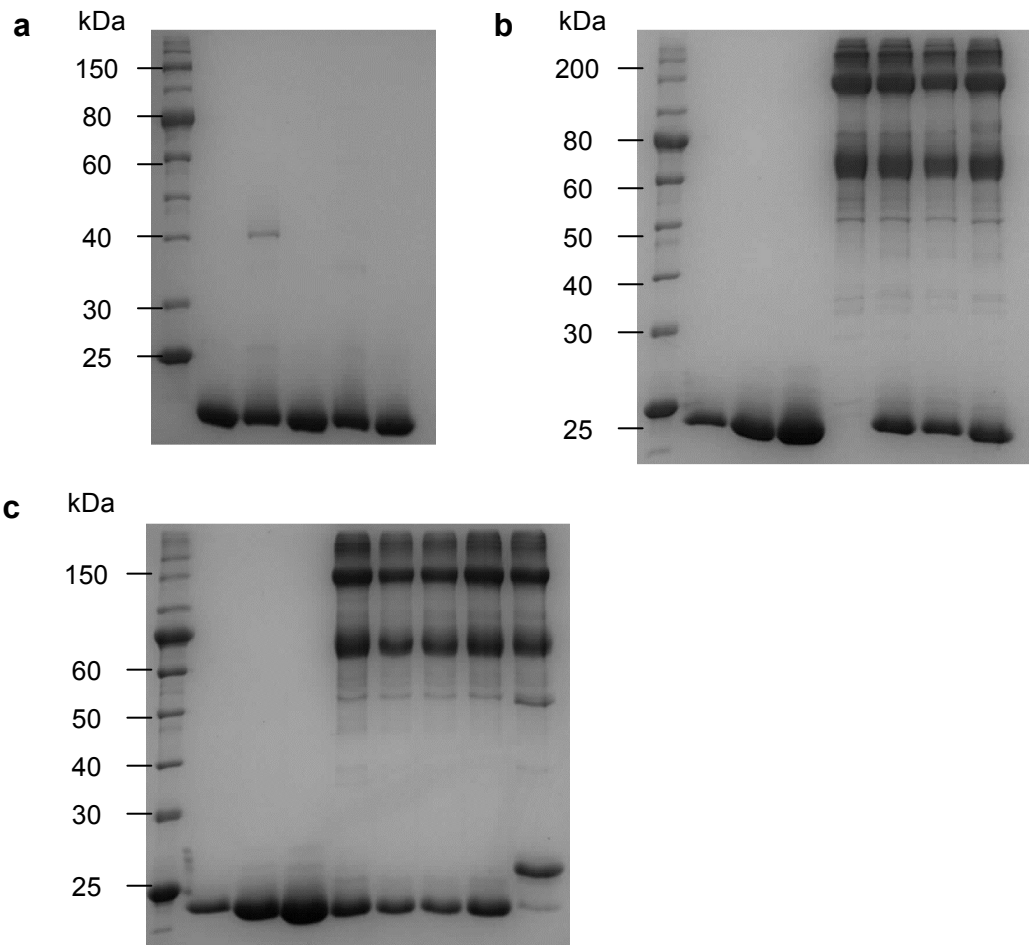


### Supplementary Figure S15: First derivative thermal denaturation fits



**a)** First derivative plots of Fig. S3I (thermal denaturation plots). MP-sscFv (blue trace – without NA1, dashed blue trace – with NA1) and MP-sscFv-SM3E (red trace – without NA1, dashed red trace – with NA1) show shifts of 9 and 13 K, respectively.  
**b)** First derivative plots of Fig. S3m (thermal denaturation plots). McP-sscFv (blue trace – without NA1, dashed blue trace – with NA1) and McP-sscFv-SM3E (red trace – without NA1, dashed red trace – with NA1) show shifts of 9 and 16 K, respectively.

**Supplementary Figure S16: Full-length gels**



**a)** Full-length gel Fig. 1c.  
**b)** Full-length gel Fig. 1h incubation in plasma 1–24 h (left).  
**c)** Full-length gel Fig. 1h incubation in human plasma 3–7 d (right).

**Supplementary Table S1: Rotational correlation times extracted by simulation and  $K_d$  values extracted using least squares fitting.**

sscFv analogue : antigen	Matrix - sscFv concentration	<sup>a</sup> T <sub>C Mobile</sub> (ns)	<sup>b</sup> T <sub>C Immo- bile</sub> (ns)	Source of data	‡K <sub>d</sub> - (μM)	‡R <sup>2</sup>
<b>MP-sscFv : NA1</b>	PBS - 10μM	2.5818	28.148	raw	1.911 ± 0.778	0.962
				simulation	1.216 ± 0.605	0.964
	Serum - 10μM	2.9882	14.9549	raw	4.352 ± 1.273	0.956
				simulation	3.938 ± 2.057	0.880
	Blood - 10μM	1.0079	8.5125	raw	6.462 ± 1.714	0.948
				simulation	5.628 ± 2.064	0.877
	Blood - 0.25μM	1.0079	8.5125	raw	0.148 ± 0.0395	0.939
				simulation	0.110 ± 0.0605	0.909
<b>MP-sscFv : full length CEA</b>	Blood - 0.25μM	1.0079	8.5125	raw	0.064 ± 0.0513	0.811
				simulation	0.052 ± 0.0297	0.948
<b>M<sub>C</sub>P-sscFv : NA1</b>	PBS - 10μM	0.8383	6.435	raw	5.621 ± 2.504	0.872
				simulation	3.718 ± 1.969	0.863
	Serum - 10μM	1.011	6.4661	raw	7.956 ± 1.812	0.928
				simulation	5.422 ± 1.197	0.929
	Blood - 10μM	0.932	7.7657	raw	6.825 ± 2.475	0.919
				simulation	5.589 ± 2.456	0.903
	Blood - 0.25μM	1.0612	3.9829	raw	0.151 ± 0.0882	0.836
				simulation	0.124 ± 0.0745	0.913
<b>M<sub>C</sub>P-sscFv : full length CEA</b>	Blood - 0.25μM	1.0612	3.9829	raw	0.074 ± 0.0471	0.860
				simulation	0.055 ± 0.0175	0.983

<sup>a</sup> T<sub>C Mobile</sub> shows the rotational correlation time estimated with Easyspin<sup>1</sup> and used to simulated weighting for simulated binding curves.

<sup>b</sup> T<sub>C Immobile</sub> is the same as <sup>a</sup> but for the simulated immobile component.

‡ K<sub>d</sub> and respective R<sup>2</sup> values were acquired using Supplementary Equation S1.

**Supplementary Table S2: Thermal denaturation melting temperatures and enthalpies of unfolding**

<b>sscFv and label type</b>	<b>T<sub>m</sub> (K)</b>	<b>ΔH unfolding (Kcal mol<sup>-1</sup>)</b>	<b>T<sub>m</sub> + NA1 (K)</b>	<b>ΔH unfolding + NA1 (Kcal mol<sup>-1</sup>)</b>
<b>MP-sscFv</b>	319.4 ± 2.3	18.48 ± 3.8	328.0 ± 1.4	36.1 ± 8.7
<b>MP-sscFv-SM3E</b>	318.3 ± 2.0	21.4 ± 4.0	331.4 ± 2.1	31.0 ± 9.8
<b>M<sub>C</sub>P-sscFv</b>	319.5 ± 1.6	20.4 ± 3.0	326.9 ± 0.9	42.9 ± 8.2
<b>M<sub>C</sub>P-sscFv-SM3E</b>	316.7 ± 1.5	11.93 ± 2.4	330.5 ± 1.9	31.9 ± 9.3

## Supplementary Equation S1: Law of mass action fitting function

Derived from the law of mass action:

$$f_B = \frac{([L] + [B]_i + K_d) - \sqrt{([L] + [B]_i + K_d)^2 - 4[L][B]_i}}{2[B]_i} \quad (1)$$

Where  $f_B$  is the fraction bound,  $[L]$ , ligand concentration,  $[B]_i$ , initial antibody concentration,  $K_d$ , dissociation constant.

## Supplementary Equation S2: Thermal denaturation fitting function

$$\frac{1}{1 + e^{-\left[\frac{\Delta H}{R}\left(\frac{1}{T} - \frac{1}{T_m}\right)\right]}} \quad (2)$$

Where  $\Delta H$  is the enthalpy of unfolding,  $R$ , universal gas constant,  $T$ , temperature,  $T_m$ , melting temperature<sup>2</sup>.

## Supplementary Methods

### General Methods

LC-MS was performed on protein samples using a Waters Acquity UPLC connected to Waters Acquity Single Quad Detector [column, Acquity UPLC BEH C18 1.7  $\mu\text{m}$  2.1  $\times$  50 mm; wavelength, 254 nm; mobile phase, 95 : 5 water (0.1% formic acid) : MeCN (0.1% formic acid), gradient over 4 min to 5 : 95 water (0.1% formic acid) : MeCN (0.1% formic acid); flow rate, 0.6 mL min<sup>-1</sup>; MS mode, ES+/-; scan range,  $m/z$  = 95–2000; scan time, 0.25 s]. Data was obtained in continuum mode. Sample volume was 30  $\mu\text{l}$  and injection volumes were 3–9  $\mu\text{l}$  with partial loop fill. The electron spray source of the MS was operated with a capillary voltage of 3.5 kV and a cone voltage of 20–200 V. Nitrogen was used as the nebulizer and desolvation gas at a total flow of 600 L h<sup>-1</sup>. Total mass spectra were reconstructed from the ion series using the MaxEnt 1 algorithm pre-installed on MassLynx software (Waters).

Relative quantification of MS data was carried out by normalisation of all identifiable peptide or protein signals (starting material, product, side and degradation products) to 100% according to their unmodified signal strength (relative ion count).

Absorbance measurements were carried out on a Carry Bio 100 (Varian) UV/ Vis spectrophotometer equipped with a temperature-controlled 12x sample holder in quartz cuvettes (1 cm path length, volume 75  $\mu\text{l}$ ) at 25 °C. Samples were baseline corrected and slits set to 5 nm. Protein solutions were scanned from 450 – 250 nm and concentration calculated using the molar extinction coefficients (based on the amino acid sequence via the ProtParam tool of the ExpASY data base; <http://expasy.org/sprot/>) with Lambert Beers law.

Reducing and non-reducing and SDS-PAGE was performed following standard lab procedures. Proteins from 20 kDa to 80 kDa were separated on 16% gels; proteins above 80 kDa were separated on 12% gels. In both cases a 4% stacking gel was used and a broad-range MW marker (10 kDa–250 kDa, BioLabs) was co-run to estimate protein weights. Samples were usually not boiled but the loading buffer contained 10% SDS. All gels were stained following a modified literature protocol<sup>3</sup>, where 0.12% of the Coomassie G-250 and the Coomassie R-250 dyes were added to the staining solution instead of only the G-250 dye.

All buffer solutions were prepared with double-deionised water and filter-sterilised. Ultrapure DMF was purchased from Sigma-Aldrich and kept under dry conditions. Opened bottles of benzeneselenol were kept under argon and replaced when the solution had turned orange. All reducing agents, dibromomaleimide and maleimide were purchased from Sigma-Aldrich.

### Reduction study of the sscFv

To the CEA-specific sscFv were added 50 equiv of TCEP, 2-mercaptoethanol, DTT, thiophenol or benzeneselenol. The reactions were maintained at ambient temperature for 2, 4 or 6 h and after the incubation period 100 equiv of monobromomaleimide were added for 20 min. All samples were analysed by LC-MS. While DTT reduced the disulfide bond of the antibody fragment efficiently, partial reduction could be observed with benzeneselenol and only weak reduction in the case of the other reducing agents.

### FPLC analysis of the sscFv

Bridged CEA-specific sscFv was synthesised either sequential or *in situ* as described. Processed sscFv was prepared by mixing the antibody fragment with DMF

(10% vol/vol) and dithiophenolmaleimide (15 equiv) and incubation for 1 h. All samples were purified on PD MiniTrap G-25 desalting columns, concentrated and 0.3 mg loaded on a HiLoad 16/26 Superdex 75 column (GE Healthcare) equilibrated in PBS. Analysis was performed at ambient temperature with a flow rate of 1.5 ml min<sup>-1</sup> and at a wavelength of 280 nm.

### **ELISA with the sscFv and its analogues**

96-well plates were coated with full length human CEA (1 µg ml<sup>-1</sup> in PBS, Calbiochem) for 1 h at ambient temperature, washed and blocked over night at 4 °C with a 5% solution of Marvel milk powder (Premier Foods) in PBS. The plates were washed and the sscFv and its analogues were added after dilution to the indicated concentrations (typically 5.0, 1.0, 0.5, 0.1, 0.05 and 0.01 µg ml<sup>-1</sup>) in PBS. The assays were incubated at ambient temperature for 1 h, washed and the primary antibody (anti-tetra-His mouse IgG1, Quiagen, 1:1000 in 1% Marvel solution) added. After 1 h at ambient temperature the ELISA plates were washed and the secondary antibody (ECL anti-mouse sheep IgG1 HRP linked, GE Healthcare, 1:1000 in 1% Marvel solution) added for 1 h at ambient temperature. The plates were washed again and freshly prepared substrate solution (one tablet of o-phenylenediamine in 25 ml 50 µM phosphate citrate buffer, Sigma-Aldrich) was added to each well. The reaction was stopped by addition of 4 M HCl and the plates read at a wavelength of 490 nm. Controls were included in every ELISA where PBS had been added to some of the wells instead of CEA or instead of the antibody fragment. Each sample was tested in triplicates.

### **Biacore measurements**

Bridged sscFv and PEG-sscFv were prepared via the *in situ* protocol, purified as described and the concentrations were determined by UV/Vis spectroscopy. The binding activity was then tested alongside unmodified sscFv, which had been processed as the functionalised analogues, via surface plasmon resonance on a Biacore T100. In brief a SA chip (coated with streptavidin) was loaded with 566 AU of biotynilated NA1 and serial dilutions of the antibody fragment and its analogues were injected (400, 200, 100, 50, 25, 12.5 and 0 nM). The contact time was 120 s at a flow rate of 20 µl min<sup>-1</sup> followed by dissociation time of 600 s. The chip was regenerated with a 10 mM glycine solution for 60 s at a flow rate of 30 µl min<sup>-1</sup>. All sample runs were performed at 25 °C and binding parameters were calculated using the provided software package (Biacore T100 Evaluation Software V 2.0.3).

### **Synthesis of alkylated sscFv**

The CEA-specific sscFv was reduced with 20 equiv of DTT for 1 h at ambient temperature. Then 50 equiv of maleimide (in DMF) were added for 10 min and the reaction analysed by LC-MS. The alkylated sscFv was purified and concentrations determined as described.

### **Stability of bridged sscFv in human plasma**

Bridged sscFv was prepared via the *in situ* protocol, purified and the concentration determined as described.

70 µg of the sscFv analogue were added to 500 µl of human plasma (Sigma-Aldrich) and incubated at 37 °C for 1 h, 4 h, 24 h, 3 d, 5 d or 7 d. The antibody fragment was purified from plasma using PureProteome Nickel Magnetic Beads (Millipore) according to manufacturers' instructions with a few exceptions: the beads were washed 4 times in wash buffer containing no imidazole and the protein eluted twice in 500 mM



imidazole for 5 min. Imidazole was removed and the eluate concentrated by repeated washes in PBS in ultrafiltration spin columns (MWCO 5 kDa, Sartorius). The protein solution was analysed by LC-MS and SDS-PAGE.

As a control alkylated sscFv was prepared as described and 25 µg of this material were mixed with 25 µg of unmodified and 25 µg of bridged anti-CEA. The mixture was added to 500 µl of PBS or human plasma, incubated for 1 h at 37 °C and purified with nickel magnetic beads as outlined above. The purified mixtures were analysed by SDS-PAGE and LC-MS to ensure a similar performance of the nickel magnetic beads for all sscFv analogues (which was observed). Alternatively alkylated or unmodified anti-CEA were incubated in human plasma at 37 °C for 7 d and isolated and analysed as described. Loss of the succinimides and subsequent reformation of the cystine was observed by LC-MS and SDS-PAGE under these conditions, a phenomenon which has been described recently<sup>4-6</sup>.

### **Activity of sscFv analogues in human plasma**

Bridged sscFv and PEG-sscFv were synthesised via the *in situ* protocol and alkylated sscFv was synthesised as described. All analogues were purified and the concentration determined as described.

37.5 µg of the antibody fragment or its analogues were added to 500 µl of human plasma and incubated at 37 °C. 12 µl were withdrawn from each sample after 1 h, 4 h, 24 h, 3 d, 5 d and 7 d, diluted in 788 µl PBS (to yield an assumed concentration of 1.1 µg ml<sup>-1</sup>), frozen in liquid nitrogen and stored at -20 °C. After all samples had been collected an ELISA assay was performed as described. As a control a dilution of human plasma in PBS was co-run, which gave no background signal.

### **Stability of the maleimide bridge against reducing agents**

Bridged sscFv was prepared via the *in situ* protocol, purified and the concentration determined as described.

The modified antibody fragment (at 60 µM) was treated with 100 equiv of 2-mercaptoethanol, DTT or GSH for 48 h at ambient temperature. Aliquots were withdrawn at different time points and analysed by LC-MS. After 48 h, all samples were reacted with 200 equiv dibromomaleimide and again subjected to LC-MS. Only the material treated with DTT was found to exist in the reduced form while the other samples had already reformed the disulfide bond.

### **PEGylation of the sscFv via lysines**

To the sscFv were added 2, 5 or 10 equiv of methoxypolyethylene glycol succinate N-hydroxysuccinimide (NHS-PEG5000, in PBS, Sigma-Aldrich) and the mixtures were incubated at ambient temperature for 30 min, 2 h or 4 h after which aliquots were withdrawn and the reaction stopped by addition of glycine (final concentration 1.7 mM). All samples were analysed by SDS-PAGE. To reach complete PEGylation of the antibody fragment 18 equiv of the PEGylation reagent were added for 4 h and the reaction stopped as described.

### **Activity of different PEG-sscFv species**

Mono-PEGylated sscFv was synthesised via the described *in situ* protocol. Multi-PEGylated sscFv was prepared via reaction with NHS-PEG5000 (18 equiv for 4 h at ambient temperature). These two species were purified using nickel magnetic beads as described.

Alternatively Mono-PEGylated anti-CEA was synthesised by reaction with 2 equiv of NHS-PEG5000 for 30 min at ambient temperature and purified after stopping the reaction with glycine by size exclusion chromatography in PBS (on a HiLoad 16/60 Sephadex 75 column, GE Healthcare).

The activity of the three PEG-sscFv species was tested alongside the unmodified antibody fragment via the described ELISA assay.

### **Cell binding assay with fluorescein-sscFv**

Fluorescein-sscFv was synthesised via the sequential protocol, purified and the concentration determined as described.

Log-phase cultures of CAPAN-1 (CEA expressing cells<sup>7</sup>, cultured in DMEM, 20% FCS, 1% glutamate, 1% streptomycin) and A375 (negative control<sup>8</sup>, cultured in DMEM, 10% FCS, 1% glutamate, 1% streptomycin) cell lines were detached non-enzymatic, counted and diluted ( $3 \times 10^3$  to  $1 \times 10^5$  per well) in a 96-well plate. The cells (in their respective media) were allowed to attach for 24 h in the incubator (at 37 °C in humid atmosphere, 5 % CO<sub>2</sub>), were gently washed twice with PBS and treated with 500 ng of the fluorescent antibody ( $5 \mu\text{g ml}^{-1}$  in PBS) per well for 1 h at ambient temperature. The plate was gently washed twice with PBS, wells filled with PBS and the fluorescence read at 518 nm (excitation 488 nm, exposure time 100 ms, slits 12 nm). Cells treated with non-fluorescent sscFv or PBS only were used to determine the background. Each sample was tested in triplicates.

### **One-step ELISAs with HRP-sscFv**

Biotin-sscFv was synthesised via the sequential protocol, purified and the concentration of the protein solution was determined as described.

The biotinylated antibody fragment was incubated with a 3x excess (by mass) of a  $1.25 \text{ mg ml}^{-1}$  solution of a HRP-Strep conjugate (Invitrogen) for 1 h at ambient temperature. The disappearance of the sscFv signal in the mix on a SDS-PAGE gel was used to verify the consumption of all biotin-sscFv by coupling to the streptavidin conjugate. The HRP-sscFv conjugate was purified with nickel magnetic beads following manufacturer's instructions. The product was analysed by SDS-PAGE and its' OD<sub>280</sub> used as a (undefined) measure of quantity to prepare dilutions.

A 96-well plate was coated with various amounts of full length CEA ( $0.125 \text{ mg ml}^{-1}$  to  $4 \text{ mg ml}^{-1}$  in PBS), blocked and washed as described and incubated with 100  $\mu\text{l}$  per well of a 1:500 dilution of a OD<sub>280</sub> = 0.4 solution of the HRP-anti-CEA conjugate for 1 h at ambient temperature. Plate read-out was performed as described.

Alternatively a standard ELISA was performed with dilutions (1:100 to 1:4,000) of an OD<sub>280</sub> = 0.4 solution of the HRP-sscFv conjugate in place of the usual antibody solutions.

### **Two-step ELISA with on-plate formation of HRP-sscFv**

An ELISA plate was prepared as described and treated with the usual dilutions of biotin-sscFv. One dilution series was reacted with the described mix of primary and secondary antibody. Another series was treated with a 1:460 dilution of the HRP-Strep conjugate (in PBS, 1% Marvel, 20x assumed mass excess over the antibody) and a third series with a 1:4,600 dilution of HRP-Strep conjugate (in PBS, 1% Marvel, 2x assumed mass excess over the antibody). Incubation times were staggered so that they did not exceed 1 h at ambient temperature for any of the samples. Visualisation and read-out were performed as described.

## Simulation of EPR spectra

The MATLAB code utilising Easyspin<sup>1</sup> (v4.0.0 plug-in) was used to load EPR spectra, subtract baseline, perform baseline correction and if necessary align spectra (alignment of spectra must be done manually and is not provided by the code). EPR spectra were then normalised to their maximum. The EPR spectrum containing no antigen (unbound) and saturated EPR spectrum (bound) were simulated to extract EPR spectra of bound ( $T_{C \text{ Immobile}}$ ) and unbound ( $T_{C \text{ Mobile}}$ ) components by varying their weighting, correlation time and line-widths by non-linear least squares fitting. A-tensor values were: [ $A_{XX}$  22  $A_{YY}$  23  $A_{ZZ}$  94] MHz and g-tensor values were: [ $g_{XX}$  2.0087  $g_{YY}$  2.0066  $g_{ZZ}$  2.0026]. These two components were then fitted to all the acquired EPR spectra to extract the weightings of the bound and unbound spectra that make up each of the respective spectra using a non-linear least squares fit. Here the Levenberg-Marquardt algorithm was used. This value was then plotted against the antigen concentration and represents the simulated weightings or fraction bound or unbound.

## Data fitting process

Data was fitted using the MATLAB cftool GUI plugin. Custom equations were used in the forms of Supplementary Equation 1 for binding curve fitting and Supplementary Equation 2 for thermal denaturation fitting. Error bars were extracted from 95% confidence fits to the respective models as predicted by the cftool fitting software for data points using non-linear regression.

## Preparation of cartoons

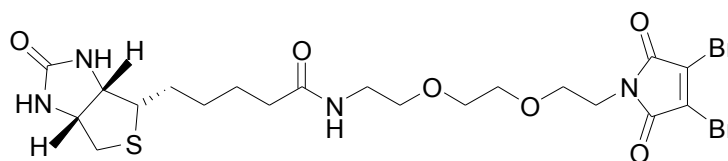
A structure of MFE23 (the parent scFv for the sscFv) bound to CEA, which was created by homology modeling and solution scattering<sup>9</sup> and which is based on the crystal structure of MFE23<sup>10</sup> (PDB code: 1QOK) was used to create the cartoons of maleimide-bridged sscFv. For the structure of the antibody fragment, residues Gly`H44 and Ala`L100 were replaced in Chimera<sup>11</sup> (University of California, San Francisco, version 1.5.3) with cysteines, their orientation corrected using the rotamer library of the software and one round of energy minimization (100 iterations, both cysteines fixed) applied with and without previous insertion of a disulfide bond.

For the antigen-bound structure, this version of MFE23diCys was super-positioned over the antibody fragment in the file and the 5 C-terminal domains of CEA as well as all inorganic atoms were removed to leave the two domains of NA1.

## Synthesis

The synthesis of dithiophenolmaleimide<sup>12</sup>, N-PEG5000-dithiophenol-maleimide<sup>12</sup> and N-fluorescein-dibromomaleimide<sup>13</sup> has been described elsewhere.

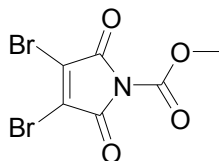
## Dibromomaleimide-N-biotin



Dibromomaleic anhydride (108.0 mg, 0.42 mmol) was added in one portion to a solution of 2-(2-(2-(5-(2-oxo-1,3,3a,4,6,6a-hexahydrothieno(3,4-d)imidazol-6-yl)pentanoylamino)ethoxy)ethoxy)ethylammonium 2,2,2-trifluoroacetate (205.0 mg, 0.42 mmol) (the preparation of these compounds has been described elsewhere<sup>14</sup>) in AcOH (10 mL) and the reaction mixture was heated to 170 °C for 2 h. Upon cooling to 21 °C toluene was added and the AcOH azeotropically removed *in vacuo*. The material was purified by flash chromatography on silica gel (methanol:dichloromethane, gradient elution from 2.0 to 7.0%) to yield the pure product as a white solid (123 mg, 48% yield).

<sup>1</sup>H NMR (600 MHz, CDCl<sub>3</sub>): δ 4.53 (dd, H, *J*=5.0, 8.0, NHC(O)NHCH), 4.34 (dd, H, *J*=5.0, 8.0, NHC(O)NHCH), 3.82 (t, 2H, *J*=5.5, OCH<sub>2</sub>), 3.70 (t, 2H, *J*=5.5, OCH<sub>2</sub>), 3.63 (m, 2H, OCH<sub>2</sub>), 3.59 (m, 2H, OCH<sub>2</sub>), 3.53 (t, 2H, *J*=5.5, NCH<sub>2</sub>), 3.37 (t, 2H, *J*=5.5, NCH<sub>2</sub>), 3.24 (dt, H, *J*=5.0, 8.0, SCH), 2.96 (dd, H, *J*=5.0, 13.0, SCHH), 2.73 (d, H, *J*=13.0, SCHH), 2.26 (t, 2H, *J*=7.5, NHC(O)CH<sub>2</sub>CH<sub>2</sub>CH<sub>2</sub>), 1.74 (m, 4H, CH<sub>2</sub>CH<sub>2</sub>CH<sub>2</sub>), 1.49 (quintet, 2H, *J*=7.5, CH<sub>2</sub>CH<sub>2</sub>CH<sub>2</sub>); <sup>13</sup>C NMR (150 MHz, CD<sub>3</sub>OD): δ 174.8 (C), 164.7 (C), 164.0 (C), 129.0 (C), 69.8 (CH<sub>2</sub>), 69.7 (CH<sub>2</sub>), 69.2 (CH<sub>2</sub>), 67.2 (CH<sub>2</sub>), 62.0 (CH), 60.2 (CH), 55.6 (CH), 39.7 (CH<sub>2</sub>), 39.0 (CH<sub>2</sub>), 38.6 (CH<sub>2</sub>), 35.4 (CH<sub>2</sub>), 28.4 (CH<sub>2</sub>), 28.1 (CH<sub>2</sub>), 25.5 (CH<sub>2</sub>); IR (solid, cm<sup>-1</sup>): 2970 (w), 1724 (s), 1365 (m), 1217 (s); Mass calc. for C<sub>20</sub>H<sub>28</sub>N<sub>4</sub>O<sub>6</sub>NaSBr<sub>2</sub>: 631.9916. Found 631.9937; m.p. 100-102 °C.

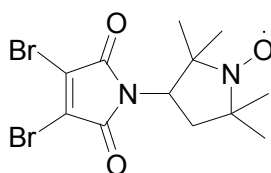
### 3,4-Dibromo-2,5-dioxo-2,5-dihydro-pyrrole-1-carboxylic acid methyl ester



To dibromomaleimide (1.0 g, 3.9 mmol) and N-methyl morpholine (433 μl, 3.9 mmol) in THF (35 ml) was added methyl chloroformate (304.0 μl, 3.9 mmol). The reaction was stirred for 20 min at ambient temperature. The solid was dissolved in dichloromethane (40 ml) and the solution was washed with water (4x 50 ml), dried with sodium sulphate and the solvent removed *in vacuo* to yield the product as a pink powder (1.03 g, 84%).

<sup>1</sup>H NMR (500 MHz, CDCl<sub>3</sub>): δ = 4.00 (s, 3H, CH<sub>3</sub>); <sup>13</sup>C NMR (125 MHz, CDCl<sub>3</sub>): δ = 159.4 (C), 147.1 (C), 131.6 (C), 55.0 (CH<sub>3</sub>); IR (solid, cm<sup>-1</sup>): 3020 (s), 1780 (m), 1735 (m); MS (CI) *m/z*, (%): 315 (<sup>81,81</sup>M<sup>+</sup>, 8), 313 (<sup>79,81</sup>M<sup>+</sup>, 19), 311 (<sup>79,79</sup>M, 11), 255 (59), 205 (100); Mass calc. for C<sub>6</sub>H<sub>3</sub>O<sub>4</sub>N<sup>79</sup>Br<sub>2</sub>: 310.8423. Found: 310.8427; m.p. 156-158 °C.

### Dibromomaleimide-N-PROXYL spin label

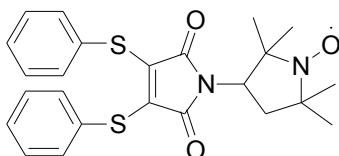


To 3,4-Dibromo-2,5-dioxo-2,5-dihydro-pyrrole-1-carboxylic acid methyl ester (441.9 mg, 1.9 mmol) in DCM (20 ml) was slowly added 3-amino-2,2,5,5-tetramethyl-1-pyrrolidinyloxy (144.0 mg, 0.9 mmol) in DCM (5 ml) and the reaction was stirred for 60 min at ambient temperature. The solvent was removed *in vacuo* and the residual material was purified by flash chromatography on silica gel (methanol:dichloromethane, gradient elution from 0.0 to 4.0%) to afford the product as an impure mixture. The material was re-purified by flash chromatography on silica gel (petroleum ether:diethyl ether, gradient elution from 9:1 to 7:3) to afford the product as a brown powder (186 mg, 50%).

$^1\text{H}$  NMR (500 MHz,  $\text{CDCl}_3$ , crude data after treatment with hydrazobenzene\*):  $\delta$  = 4.51 (dd, H,  $J=11.3$ , 8.8, CH), 2.92 (appt. t, H,  $J=12.2$ ,  $\text{CH}_2$ ), 1.84 (dd, H,  $J=12.9$ ,  $J=8.7$ ,  $\text{CH}_2$ ), 1.38 (s, 3H,  $\text{CH}_3$ ), 1.28 (s, 3H,  $\text{CH}_3$ ), 1.26 (s, 3H,  $\text{CH}_3$ ), 1.11 (s, 3H,  $\text{CH}_3$ );  $^{13}\text{C}$  NMR (125 MHz,  $\text{CDCl}_3$ , crude data after treatment with hydrazobenzene\*):  $\delta$  = 164.4 (C), 129.7 (C), 57.1 (CH), 35.7 ( $\text{CH}_2$ ), 27.2 (C), 25.6 (C), 25.2 (2x  $\text{CH}_3$ ), 21.6 (2x  $\text{CH}_3$ ); IR (solid,  $\text{cm}^{-1}$ ): 2975 (w), 2934 (w), 1785 (w), 1722 (s), 1603 (m); MS (EI)  $m/z$ , (%): 397 ( $^{81,81}\text{M}^+$ , 12), 395 ( $^{79,81}\text{M}^+$ , 22), 393 ( $^{79,79}\text{M}$ , 12), 309 (100); Mass calc. for  $\text{C}_{12}\text{H}_{15}\text{O}_3\text{N}_2^{79}\text{Br}_2$ : 392.9444. Found: 392.9440; m.p. 171-176 °C.

\*In order to obtain detailed NMR spectra it was necessary to reduce the PROXYL radical prior to NMR-spectroscopy. This was done by treatment of the purified spin label with a 3x excess (by mass) of hydrazobenzene for 60 min. The presented data is thus an excerpt of the mixture of the spin label, hydrazobenzene and their reaction products.

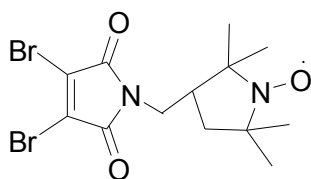
### Dithiophenolmaleimide-N-PROXYL spin label (TPMP)



To the dibromomaleimide-N-PROXYL spin label (100.0 mg, 0.3 mmol) and sodium hydrogencarbonate (107.1 mg, 1.3 mmol) in methanol (35 ml) was slowly added benzenethiol (52.2  $\mu\text{l}$ , 0.6 mmol) in methanol (5 ml). The reaction was stirred for 10 min at ambient temperature. The solvent was removed *in vacuo* and the residual material was purified by flash chromatography on silica gel (petroleum ether:ethyl acetate, gradient elution from 9:1 to 7:3) to afford the product as an orange powder (79 mg, 68%).

$^1\text{H}$  NMR (500 MHz,  $\text{CDCl}_3$ , crude data after treatment with hydrazobenzene\*):  $\delta$  = 7.35-7.19 (m, 10H, Ar-H), 4.29 (dd, H,  $J=11.9$ , 7.3, CH), 3.00 (dd, H,  $J=10.2$ , 7.6,  $\text{CH}_2$ ), 2.04 (dd, H,  $J=12.5$ ,  $J=7.4$ ,  $\text{CH}_2$ ), 1.31 (s, 3H,  $\text{CH}_3$ ), 1.23 (s, 3H,  $\text{CH}_3$ ), 1.21 (s, 3H,  $\text{CH}_3$ ), 1.08 (s, 3H,  $\text{CH}_3$ );  $^{13}\text{C}$  NMR (125 MHz,  $\text{CDCl}_3$ , crude data after treatment with hydrazobenzene\*):  $\delta$  = 167.4 (C), 136.0 (C), 132.4 (CH), 131.9 (CH), 131.1 (CH), 129.4 (C), 56.3 (CH), 35.5 ( $\text{CH}_2$ ), 27.3 (C), 25.7 (C), 24.9 (2x  $\text{CH}_3$ ), 21.9 (2x  $\text{CH}_3$ ); IR (solid,  $\text{cm}^{-1}$ ): 2973 (w), 2930 (w), 1771 (w), 1708 (s), 1631 (w), 1582 (w), 1537 (w); MS (EI)  $m/z$ , (%): 453 (M, 17), 99 (100); Mass calc. for  $\text{C}_{24}\text{H}_{25}\text{O}_3\text{N}_2\text{S}_2$ : 453.1307. Found: 453.1292; m.p. 124-128 °C.

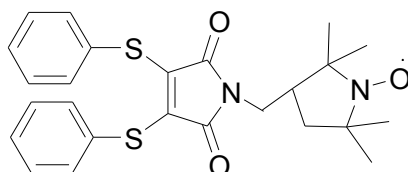
### Dibromomaleimide-N-methyl-PROXYL spin label



To 3,4-Dibromo-2,5-dioxo-2,5-dihydro-pyrrole-1-carboxylic acid methyl ester (274.6 mg, 0.9 mmol) in DCM (20 ml) was slowly added 3-(aminomethyl)-PROXYL (75.0 mg, 0.4 mmol) in DCM (3 ml) and the reaction was stirred for 24 h at ambient temperature. The solvent was removed *in vacuo* and the residual material was purified by flash chromatography on silica gel (petroleum ether:diethyl ether, gradient elution from 9:1 to 0:1) to afford the product as a brown powder (132 mg, 73%).

$^1\text{H}$  NMR (500 MHz,  $\text{CDCl}_3$ , crude data after treatment with hydrazobenzene\*):  $\delta$  = 3.68 (dd, H,  $J=13.8$ , 7.9, CHH), 3.53 (dd, H,  $J=14.6$ , 10.3, CHH), 2.17-2.01 (m, H, CH), 1.70 (dd, H,  $J=12.8$ ,  $J=7.7$ ,  $\text{CH}_2$ ), 1.60 (appt. t, H,  $J=11.7$ ,  $\text{CH}_2$ ), 1.22 (s, 6H, 2x $\text{CH}_3$ ), 1.15 (s, 3H,  $\text{CH}_3$ ), 1.09 (s, 3H,  $\text{CH}_3$ );  $^{13}\text{C}$  NMR (125 MHz,  $\text{CDCl}_3$ , crude data after treatment with hydrazobenzene\*):  $\delta$  = 164.0 (C), 129.6 (C), 42.5 (CH), 40.9 (CH $_2$ ), 40.4 (CH $_2$ ), 28.2 (C), 26.3 (C), 26.2 (2x  $\text{CH}_3$ ), 25.7 (2x  $\text{CH}_3$ ); IR (solid,  $\text{cm}^{-1}$ ): 2971 (w), 2933 (w), 1784 (w), 1718 (s), 1696 (m); MS (EI)  $m/z$ , (%): 411 ( $^{81,81}\text{M}^+$ , 21), 409 ( $^{79,81}\text{M}^+$ , 46), 407 ( $^{79,79}\text{M}$ , 21), 323 (100), 308 (36), 268 (58); Mass calc. for  $\text{C}_{13}\text{H}_{17}\text{O}_3\text{N}_2^{79}\text{Br}_2$ : 406.9600. Found: 406.9596; m.p. 136-139 °C.

### Dithiophenolmaleimide-N-methyl-PROXYL spin label (TPM<sub>c</sub>P)



To the dibromomaleimide-N-methyl-PROXYL spin label (80.0 mg, 0.2 mmol) and sodium hydrogencarbonate (82.2 mg, 1.0 mmol) in methanol (30 ml) was slowly added benzenethiol (40.1  $\mu\text{l}$ , 0.4 mmol) in methanol (3 ml). The reaction was stirred for 10 min at ambient temperature. The solvent was removed *in vacuo* and the residual material was purified by flash chromatography on silica gel (petroleum ether:ethyl acetate, gradient elution from 9:1 to 7:3) to afford the product as a viscous yellow liquid (44 mg, 47%).

$^1\text{H}$  NMR (500 MHz,  $\text{CDCl}_3$ , crude data after treatment with hydrazobenzene\*):  $\delta$  = 7.33-7.26 (m, 10H, Ar-H), 3.57 (dd, H,  $J=13.8$ , 6.2, CHH), 3.41 (dd, H,  $J=14.2$ , 4.3, CHH), 2.16-2.09 (m, H, CH), 1.65 (dd, 2H,  $J=12.4$ ,  $J=7.7$ ,  $\text{CH}_2$ ), 1.55 (appt. t, H,  $J=11.8$ ,  $\text{CH}_2$ ), 1.18 (s, 3H,  $\text{CH}_3$ ), 1.16 (s, 3H,  $\text{CH}_3$ ), 1.12 (s, 3H,  $\text{CH}_3$ ), 1.02 (s, 3H,  $\text{CH}_3$ );  $^{13}\text{C}$  NMR (125 MHz,  $\text{CDCl}_3$ , crude data after treatment with hydrazobenzene\*):  $\delta$  = 166.8 (C), 136.0 (C), 132.0 (CH), 131.1 (CH), 129.4 (C), 128.6 (CH), 41.9 (CH), 40.9 (CH $_2$ ), 39.9 (CH $_2$ ), 29.1 (CH $_3$ ), 26.6 (CH $_3$ ), 26.5 (CH $_3$ ), 23.9 (CH $_3$ ); IR (solid,  $\text{cm}^{-1}$ ): 2971 (w), 2932 (w), 1737 (w), 1704 (s), 1581 (w); MS (EI)  $m/z$ , (%): 467 (M, 44),

326 (55), 161 (47), 110 (100) Mass calc. for C<sub>25</sub>H<sub>27</sub>O<sub>3</sub>N<sub>2</sub>S<sub>2</sub>: 467.1458. Found: 467.1462.

## References

1. Stoll, S. & Schweiger, A. EasySpin, a comprehensive software package for spectral simulation and analysis in EPR. *J. Magn. Reson.* **178**, 42-55 (2006).
2. Layton, C. J. & Hellinga, H. W. Thermodynamic analysis of ligand-induced changes in protein thermal unfolding applied to high-throughput determination of ligand affinities with extrinsic fluorescent dyes. *Biochemistry* **49**, 10831-10841.
3. Candiano, G. *et al.* Blue silver: a very sensitive colloidal Coomassie G-250 staining for proteome analysis. *Electrophoresis* **25**, 1327-1333 (2004).
4. Fishkin, N., Maloney, E. K., Chari, R. V. & Singh, R. A novel pathway for maytansinoid release from thioether linked antibody-drug conjugates (ADCs) under oxidative conditions. *Chem. Commun. (Camb.)* **47**, 10752-10754 (2011).
5. Baldwin, A. D. & Kiick, K. L. Tunable degradation of maleimide-thiol adducts in reducing environments. *Bioconjug. Chem.* **22**, 1946-1953 (2011).
6. Shen, B. Q. *et al.* Conjugation site modulates the in vivo stability and therapeutic activity of antibody-drug conjugates. *Nat. Biotechnol.* **30**, 184-189 (2012).
7. el-Deriny, S. E., O'Brien, M. J., Christensen, T. G. & Kupchik, H. Z. Ultrastructural differentiation and CEA expression of butyrate-treated human pancreatic carcinoma cells. *Pancreas* **2**, 25-33 (1987).
8. Lisy, M. R. *et al.* In vivo near-infrared fluorescence imaging of carcinoembryonic antigen-expressing tumor cells in mice. *Radiology* **247**, 779-787 (2008).
9. Boehm, M. K. & Perkins, S. J. Structural models for carcinoembryonic antigen and its complex with the single-chain Fv antibody molecule MFE23. *FEBS Lett.* **475**, 11-16 (2000).
10. Boehm, M. K. *et al.* Crystal structure of the anti-(carcinoembryonic antigen) single-chain Fv antibody MFE-23 and a model for antigen binding based on intermolecular contacts. *Biochem. J.* **346 Pt 2**, 519-528 (2000).
11. Pettersen, E. F. *et al.* UCSF Chimera--a visualization system for exploratory research and analysis. *J. Comput. Chem.* **25**, 1605-1612 (2004).
12. Schumacher, F. F. *et al.* In situ maleimide bridging of disulfides and a new approach to protein PEGylation. *Bioconjug. Chem.* **22**, 132-136 (2011).
13. Smith, M. E. *et al.* Protein modification, bioconjugation, and disulfide bridging using bromomaleimides. *J. Am. Chem. Soc.* **132**, 1960-1965 (2010).
14. Ryan, C. P. *et al.* Tunable reagents for multi-functional bioconjugation: reversible or permanent chemical modification of proteins and peptides by control of maleimide hydrolysis. *Chem. Commun. (Camb.)* **47**, 5452-5454 (2011).